Exploring the adhesion mechanisms of human peripheral blood monocytes onto oxygen and nitrogen-rich gradient plasma polymer-coated fluoropolymers

Jiyu (Jessica) Tian

Department of Chemical Engineering
McGill University
Montréal, Québec, Canada
November 2022

A thesis submitted to McGill University in partial fulfillment of the requirements for the degree of

Master of Science

ABSTRACT

Dendritic cell (DC)-based immunotherapy is a promising strategy to treat malignant diseases. Traditionally, DCs are obtained by differentiating monocytes (Mo-DCs) in open flask systems using tissue culture polystyrene (TCPS) as the substrate. Disposable culture bags composed of flexible fluoropolymers such as fluorinated ethylene propylene (FEP) represent promising alternatives to polystyrene flasks to minimize the risks of contamination when producing therapeutic cells for clinical use. The transition from the more hydrophilic TCPS (adherent culture) to the more hydrophobic fluoropolymers (suspension culture) entails significant changes in the substrate surface properties which can impact protein adsorption and cell product attributes. The impact of culture substrate materials on the cell-surface interactions and the resulting cell fate decisions of *ex vivo*-derived Mo-DCs remains to be elucidated. Despite the hydrophobicity of FEP, we previously observed monocyte adhesion to FEP through mechanisms that were unclear.

The hypothesis investigated in this thesis was that Mo-DC surface interactions can be modulated by tuning the substrate surface chemistry. To this end, we functionalized FEP with in-house-developed oxygen-rich and nitrogen-rich gradient plasma polymer coatings (GPPCs) that were generated by plasma-enhanced chemical vapor deposition (PECVD). These GPPCs introduce O- and N-containing functional groups at the substrate surface which are retained after steam sterilization and in aqueous media. We conducted studies to investigate the impact of GPPCs on monocyte adhesion as compared to conventional TCPS flasks and untreated FEP bags (referred to as FEP(-)). Monocyte initial adhesion onto O- and N-rich GPPCs was significantly enhanced as compared to FEP(-), and was comparable to TCPS (57±6%, 51±6%, 34%±6% and 54±7% of the seeded cells adhered to each surface, respectively). Immunofluorescence staining indicated that monocytes adhered to FEP(-), O- and N-rich GPPCs through focal adhesions, with the highest cell spreading being observed on O-GPPC. In addition, both GPPCs enhanced monocyte adhesion strength under tangential flow.

To probe the mechanisms of plastic adherence, we seeded monocytes in the presence of ethylenediaminetetraacetic acid (EDTA) and RGD (Arg-Gly-Asp) peptide to hinder integrin interactions with binding partners. The reduced cell adhesion indicated the involvement of integrins, especially RGD-binding integrins, in mediating monocyte adhesion to FEP substrates.

After probing different blocking strategies of integrin subunits, integrin α5/β1 (CD49e/CD29) was identified as a putative monocyte-FEP adhesion mediator based on a >50% reduction in monocyte initial adhesion.

In summary, the results presented in this thesis demonstrated the strong translational potential of the GPPCs in developing functionalized FEP bags with enhanced interactions with cells. Our improved understanding of monocyte adhesion mechanisms will inform the engineering of culture substrate materials that can be tailored towards pro-adherent or pro-suspension cultures of Mo-DCs depending on the targeted applications. This strategy could improve the *in vitro* manufacturing efficiency and *in vivo* therapeutic efficacy of Mo-DC immunotherapies.

RÉSUMÉ

L'immunothérapie basée sur les cellules dendritiques (CDs) est une stratégie prometteuse pour traiter les pathologies cancéreuses. Traditionnellement, les CDs sont obtenues par différenciation de monocytes (Mo-CD) dans des systèmes de flacons ouverts utilisant du polystyrène pour la culture tissulaire (TCPS) comme substrat. Les sacs de culture en fluoropolymères flexibles tels que l'éthylène-propylène fluoré (FEP) apportent une solution permettant la génération de thérapies cellulaires cliniques dans des environnements fermés avec un risque de contamination considérablement réduit par rapport aux systèmes ouverts. Cependant, les propriétés de surface du substrat peuvent avoir un impact considérable sur l'adsorption des protéines et les interactions entre les cellules et la surface. Le passage du TCPS hydrophile (culture adhérente) aux fluoropolymères hydrophobes (culture en suspension) entraîne des changements significatifs dans le comportement des cellules à l'interface du substrat. À ce jour, notre compréhension de l'impact de la nature du substrat sur les interactions cellule-surface et la différentiation cellulaire des Mo-CDs dérivées *ex vivo* demeure incomplète. De plus, bien que les surfaces en FEP offrent des interactions limitées avec les cellules en raison de leur caractère hydrophobe, nous avons observé l'adhésion des monocytes aux sacs en FEP par des mécanismes qui ne sont pas définis.

L'hypothèse étudiée dans cette thèse est que les interactions cellule-surface peuvent être modulées en ajustant la chimie de surface du substrat. À cette fin, nous avons fonctionnalisé le FEP avec des revêtements polymériques à gradient déposés par plasma (GPPC) riches en oxygène et en azote, générés par dépôt chimique en phase vapeur assisté par plasma (PECVD). Ces GPPCs à la chimie finement ajustée introduisent des groupements fonctionnels contenant de l'oxygène et de l'azote à la surface du substrat et leur intégrité a été vérifiée en milieu aqueux et lors de la stérilisation à la vapeur. Nous avons mené des études pour examiner l'impact des GPPCs sur le comportement d'adhésion des monocytes en les comparant aux flacons TCPS conventionnels et aux sacs en FEP non traité (appelés FEP(-)). L'adhésion initiale des monocytes sur les O- et N-GPPCs était significativement plus élevée que sur le FEP(-), et était comparable à celle observée sur le TCPS (57 ± 6%, 51 ± 6%, 34% ± 6% et 54 ± 7% des cellules ensemencées ont adhéré sur chaque surface, respectivement). La coloration par immunofluorescence a indiqué que les monocytes adhéraient aux surfaces FEP(-), O- et N-GPPC par le biais d'adhésions focales. Le nombre d'adhésions focales et l'étalement cellulaire étaient les plus élevés sur les surfaces recouvertes de O-GPPC. En outre, les deux GPPCs ont augmenté la force d'adhésion des monocytes sous flux tangentiel.

Afin d'explorer les mécanismes d'adhésion cellulaire au plastique, nous avons ensemencé des monocytes en présence de l'acide éthylènediaminetétraacétique (EDTA) et du peptide RGD (Arg-Gly-Asp). La réduction de l'adhésion cellulaire en présence du RGD indique un rôle des intégrines se liant au RGD dans les mécanismes d'adhésion des monocytes aux substrats en FEP. Un immunophénotypage complet du système d'intégrines exprimées par les monocytes et des expériences d'inhibition utilisant des anticorps monoclonaux ont été réalisés afin d'identifier plus précisément les récepteurs spécifiques impliqués dans le processus d'adhésion. Le blocage de l'intégrine α5/β1 (CD49e/CD29) a conduit à une réduction de plus de 50% de l'adhésion initiale des monocytes, confirmant son rôle clé en tant qu'intermédiaire dans l'adhésion cellulaire aux surfaces en FEP.

En résumé, les résultats présentés dans cette thèse ont démontré le fort potentiel translationnel des GPPCs dans le développement de sacs en FEP fonctionnalisés avec des interactions améliorées avec les cellules. De plus, compréhension accrue des mécanismes d'adhésion des monocytes permettra de concevoir des substrats de culture pouvant favoriser ou plutôt réduire l'adhérence cellulaire en fonction des applications visées, optimisant ainsi l'efficacité de la fabrication *in vitro* et l'efficacité thérapeutique *in vivo* des immunothérapies Mo-CD.

ACKNOWLEDGMENTS

The last two years of my master's studies have been such an enriching journey for me both personally and professionally, which would not have been possible without the tremendous support that I've received from my supervisors, collaborators, colleagues, families and friends.

I would first and foremost like to express my deepest gratitude to my supervisors, Dr. Corinne Hoesli and Dr. Pierre-Luc Girard-Lauriault. I'm immensely humbled and grateful to have been given the opportunity to become your student. Pierre-Luc, thank you for all the valuable suggestions you've given on my research and for always having faith in me. Your trust and encouragement have given me a lot of confidence and motivated me to keep on going. Corinne, I knew you since I was still an undergraduate student back in 2017. You have always been the most caring professor that I've ever met who tries to help students in every single bit you could! From bringing me into your lab, to all your invaluable input on my research, and to the long talks we had to help me map out my future path, I can't thank you enough for your never-stopping guidance and support. In addition, the professionalism and work ethic of both of you have inspired me and shaped me into the researcher I am today.

Secondly, I'd like to sincerely thank our wonderful collaborators at Saint-Gobain Research North America, Dr. Nicolas Drolet, Dr. Natalie Fekete and Dr. Katie Campbell, for all your insightful suggestions and feedback on my research. I've learned so much from you all through our collaboration which I know will take me further. A special thanks to Natalie who's an amazing collaborator and also a great mentor to me! From guiding me on my flow cytometry experiment design, to helping me explore future career opportunities, thank you Natalie for all your support along the journey! I'd also like to thank our other collaborators, Dr. Michel L. Tremlay from Kanyr Pharma, and Dr. Pierre Laneuville, Dr. Linda Peltier from the McGill University Health Center. I'm extremely honored to work with such a multidisciplinary team of top scientists and experts.

Many thanks to the Hoesli lab and PLGL lab members for being great lab mates and good friends. A big thank you to Dr. Balaji Ramachandran who is such a pleasure to work with! I'm so glad to work on the same project with you, and thanks for always being there whenever I needed help! Thank you to our fantastic lab technician Ms. Lisa Danielczak for coordinating blood donations for me and for her endless efforts to keep our lab such an organized and joyful place to work! Dr.

Nabil Zeidan, thank you for training me on blood processing and monocyte culture. Jonathan (Jonathan Brassard), thank you for helping me translate my abstract into French! And everyone else in the Hoesli lab and PLGL lab, thank you for making the past two years such a joyful experience for me!

Next, I'd like to thank our funding sources, Saint-Gobain, NSERC, MEDTEQ and MITACS for making the work presented herein possible. Thank you to FRQNT for granting me a Master's scholarship. Also, thank you to our partnering networks ThéCell, Proteo, CQMF and MRM.

Finally, I owe a debt of gratitude to my mom (Ms. Yurong Wang) and dad (Mr. Xin Tian) for their unconditional love and support at every moment, especially during my graduate studies! Thank you for always being my safe harbor. Knowing you are around has been my source of confidence and comfort whenever I face challenges. Thank you also for always giving me the wisest advice at every turning point in my life. I wouldn't be able to reach this far without you! Additionally, I'd like to thank my friends, especially my best friend Jiyuan Wu, for cheering me up and supporting me throughout my studies!

STATEMENT OF CONTRIBUTION

This thesis was solely written by me and kindly edited by my co-supervisors Dr. Corinne Hoesli and Dr. Pierre-Luc Girard-Lauriault. I personally conducted all the experiments and analyzed all the data presented in this work. I acknowledge that I received help from my colleagues on certain experiments as outlined below:

- The GPPCs were developed, characterized and optimized by Dr. Balaji Ramachandran and Dr. Gad Sabattier, and are currently under licensing discussions with Saint-Gobain[1]. Additionally, Balaji performed the surface characterization studies of the GPPCs presented in the literature review (Figure 2-5 in Section 2.3.3).
- Balaji trained me on the PECVD reactor and I conducted the plasma depositions with assistance from Balaji.
- Balaji and I conducted together the second and third experimental replicates of the monocyte initial adhesion studies on the GPPCs (results in section 4.1.1) as part of his training on monocyte culture.

Of note, the work presented herein contributed to the production of 3 internal reports submitted to industrial partners, as well as 1 first-author oral presentation and 1 first-author poster presentation. The results presented in this thesis will also lead to a first-author manuscript currently under preparation. Author contribution to the manuscript will be as follows:

- **Jiyu (Jessica) Tian**: Conceptualization, Methodology, Investigation, Formal analysis, Visualization, Writing – original draft, review and editing.
- Balaji Ramachandran: Conceptualization, Investigation, Formal analysis, Writing - review and editing.
- Natalie Fekete: Conceptualization, Writing - review and editing.
- Nicolas Drolet: Conceptualization, Writing - review and editing.
- Katie Campbell: Conceptualization, Writing - review and editing.
- Michel L. Tremlay: Conceptualization, Writing - review and editing.
- Pierre-Luc Girard-Lauriault: Conceptualization, Writing - review and editing, Supervision.
- Corinne Hoesli: Conceptualization, Writing - review and editing, Supervision, Project administration.

TABLE OF CONTENTS

List of Abbreviations

APCs	Antigen-presenting cells
CAMs	Cell adhesion molecules
CD	Cluster of differentiation
cGMP	Current good manufacturing practice
CTLs	Cytotoxic T lymphocytes
DAPI	4’,6-diamidino-2-phenylindole
DCs	Dendritic cells
DPBS	Dulbecco’s phosphate-buffered saline
ECM	Extracellular matrix
EDTA	Ethylenediaminetetraacetic acid
F-actin	Filamentous actin
FA	Focal adhesion
FAK	Focal adhesion kinase
FDA	Food and Drug Administration
FEP	Fluorinated ethylene propylene
FITC	Fluorescein isothiocyanate
FMO	Fluorescence minus one
GM-CSF	Granulocyte-macrophage colony-stimulating factor
GPPC	Gradient plasma polymer coating
HSA	Human serum albumin
HI-FBS	Heat-inactivated fetal bovine
IFN-γ	Interferon-γ
IL	Interleukin
MFI	Median fluorescence intensity
MHC	Major histocompatibility complex
MIDAS	Metal-ion-dependent adhesion site
Mo-DCs	Monocyte-derived dendritic cells
MPLA	Monophosphoryl lipid A
N-hyb-GPPC	Nitrogen-rich hybrid gradient plasma polymer coating
O-GPPC	Oxygen-rich gradient plasma polymer coating
PBMCs	Peripheral blood mononuclear cells
PECVD	Plasma-enhanced chemical vapor deposition
RF	Radio frequency

RGD	Arginylglycylaspartic acid (Arg-Gly-Asp)
RO	Reverse osmosis
RPMI	Roswell Park Memorial Institute
TAAs	Tumor-associated antigens
TCPS	Tissue culture polystyrene
TCR	T-cell receptor
TRITC	Tetramethylrhodamine
WST-8	Water-soluble tetrazolium 8
XPS	X-ray photoelectron spectroscopy

List of Tables

List of Figures

1 INTRODUCTION

The pivotal role played by dendritic cells (DCs) in the crosstalk and regulation of the innate and adaptive immune systems makes them a promising vehicle for a plethora of indications including the treatment of cancer. DC-based cancer immunotherapies harness the antigen-presenting ability of DCs to reengage the immune system's anti-tumor responses after being administered to the patient. The production of DC-based immunotherapies requires the *in vitro* differentiation and maturation from their progenitors, most commonly peripheral blood primary monocytes. While tissue culture polystyrene (TCPS) constitutes the conventional substrate material for *in vitro* cell culture, vessels made of TCPS such as T-flasks and multiwell plates adopt an open configuration which introduces risks of contamination. In the context of production of clinical cellular therapies in accordance with current good manufacturing practice (cGMP) regulations, single-use fluoropolymer bags such as the Saint-Gobain VueLife® series composed of fluorinated ethylene propylene (FEP) are preferred due to the greatly minimized risks of contamination in closed manufacturing systems. The excellent polymer properties of FEP such as good gas permeability, minimal evaporative water loss and chemical resistance have made it an exciting material for vessel design. In addition, FEP culture bags can be easily scaled up (to produce broadly applicable therapeutic products), or scaled out (to produce personalized, patient-tailored therapies) owing to the mechanical flexibility of FEP.

However, transitioning from adherent cultures in polystyrene flasks to suspension cultures in fluoropolymer bags entails significant changes in the vessel material properties, which could impact protein adsorption and cell-substrate interactions. The effects of selecting FEP over polystyrene on the cell fate decisions of Mo-DCs have been reviewed elsewhere[2]. Most authors reported no significant differences between Mo-DCs generated in bags versus flasks[3–5], whereas some studies demonstrated diminished functional abilities of bag-generated Mo-DCs cultured in suspension[6]. In addition, the facultative adherent nature of monocytes makes it challenging to predict their behavior upon contact with the substrate surface. In spite of the intrinsic hydrophobicity and bio-inertness of FEP, we and others observed monocyte and Mo-DC adhesion onto FEP[5,6], a phenomenon hardly seen with anchorage-dependent cell types such as human mesenchymal stromal cells. Whether monocyte adhesion to plastic affects their differentiation and maturation into Mo-DCs has not yet been revealed. To explore this scientific question, we must

identify the underlying mechanisms governing monocyte interactions with hydrophobic surfaces such as FEP, which however, still remain poorly understood.

In general, protein adsorption happens within a much faster timeframe than cell adhesion upon contact with a solid substrate[7]. Therefore, cell-surface adhesion is likely to be mediated by interactions between surface-adsorbed proteins and cell adhesion molecules (CAMs)[7]. In particular, integrins are widely recognized as the primary cell-surface adhesion mediators among all CAMs[8,9]. Numerous studies have demonstrated that substrate surface properties impose a determining control over the protein adsorption phenomena, which consequently controls the behavior of various cell types when they come into contact with the surface [10–13]. Interestingly, a few authors observed that hydrophilic surfaces favored the adsorption of pro-adhesion proteins (such as common extracellular matrix (ECM) proteins fibronectin and vitronectin), whilst hydrophobic substrates were found to promote adsorption of globular proteins (such as albumin) which are adhesion-inhibiting[10,11].

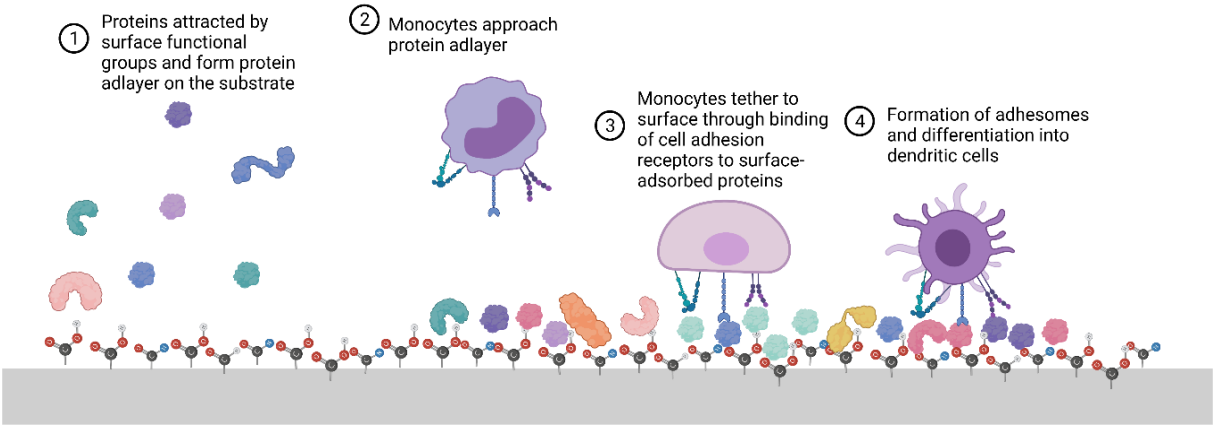

Figure 1-1 Hypothesized mechanisms of cell-protein-surface interactions at play in monocyte initial adhesion and differentiation into Mo-DCs. Created with BioRender

Hence, our overall objective was to identify the underlying mechanisms governing monocyte adhesion onto FEP. We hypothesized that integrins are implicated in monocyte-FEP interactions, and by tuning the surface chemistry of FEP, we can modulate the extent of monocyte adhesion mediated through integrin-dependent mechanisms. To this end, we employed plasma-enhanced chemical vapor deposition (PECVD) to functionalize hydrophobic FEP with oxygen-rich or nitrogen-rich gradient plasma polymer coatings (GPPCs)[1]. Plasma polymerization is a surface modification technique to render inert polymer substrates more bio-active and bio-compatible[14].

In this context, a thin layer of organic coating containing biologically relevant chemical functionalities such as amine (for N-rich GPPC) and carboxyl groups (for O-rich GPPC) is deposited on FEP, permitting tuning of the base substrate with desirable surface chemistries to tailor cell-surface interactions.

The overall objective was divided into two sub-aims:

1) Studying monocyte initial adhesion behavior on GPPC-treated FEP substrates in comparison to commercially available culture dishes, namely Sarstedt TCPS (referred to as TCPS(+)), FEP bags sold for adherent culture (Saint-Gobain VueLife® AC Series, referred to as FEP(+)) and untreated FEP bags for suspension culture (Saint-Gobain VueLife® C Series, referred to as FEP(-)).
2) Probing the mechanisms by which monocytes adhere to FEP-based substrates and the extent to which adhesion mechanisms were impacted by surface properties.

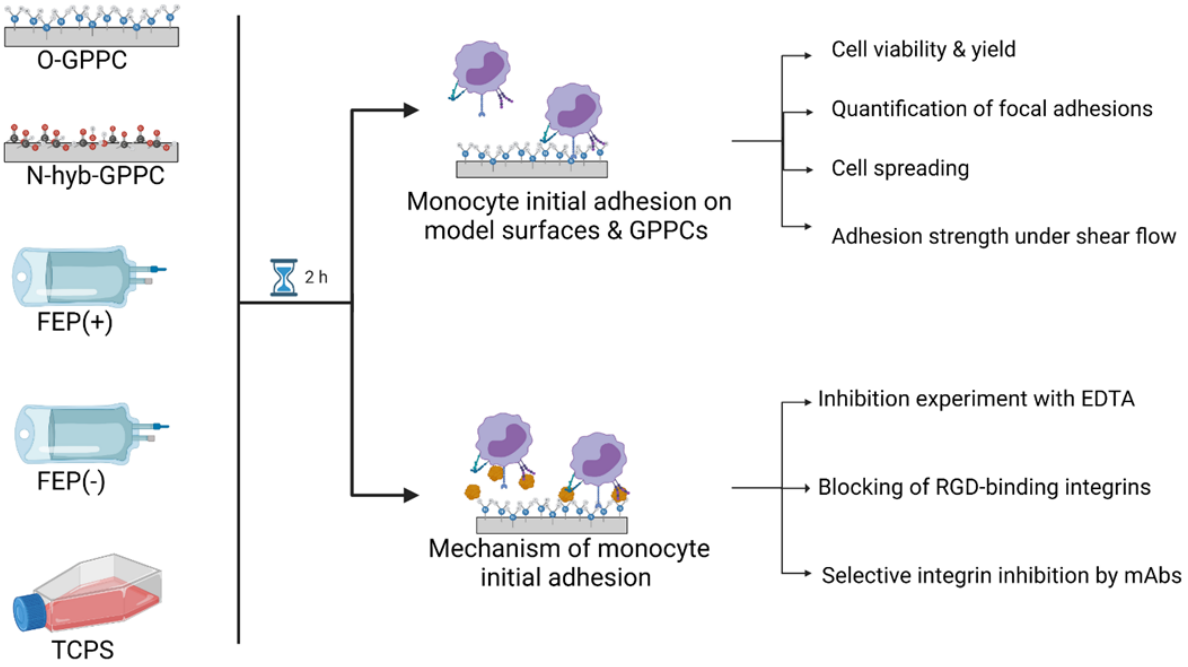

Figure 1-2 Overview of experiments conducted in this thesis.Created with BioRender

2 LITERATURE REVIEW

2.1 Introduction to Mo-DC cancer immunotherapy

Since their discovery by Cohn and Steinman in 1973[15], DCs have been widely recognized as the most potent professional antigen-presenting cells (APCs). While other APC populations such as macrophages and B cells also possess the ability to uptake and process antigens, DCs, however, are the only cell type in circulation capable of migrating to the lymph nodes to activate naïve T cells, thus serving as the bridge between the innate and adaptive immunity[16,17]. The pivotal function of DCs to initiate antigen-specific adaptive immunity has positioned it at the fulcrum of the regulation of the immune systems, which makes DCs a potent vaccination platform to treat diseases that do not respond to conventional treatments.

DC-based immunotherapies have been applied to treat a multitude of diseases, including autoimmune disorders and chronic viral infections such as HIV, but the vast majority of its application is towards cancer treatment[18]. The goal of DC-based cancer immunotherapy is to exploit the antigen presentation capacity of DCs to reengage the tumor-specific immune responses mediated by cytotoxic T lymphocytes. It is worth noting that the first US Food and Drug Administration (FDA)-approved cellular therapy, sipuleucel-T, was a personalized, autologous DC vaccine for the treatment of advanced-stage prostate cancer[19]. Aside from the capacity to induce tumor-specific adaptive immunity, DC-based vaccines also have a favorable safety profile due to their low immune-related toxicity (e.g. risk of inducing autoimmunity) compared with other immunotherapeutic strategies such as cytokine and antibody therapies[16,20]. Altogether, the unique therapeutic potentials of DC-based vaccine have made it a promising strategy with appealing prospects in the field of cancer treatment.

2.1.1 Basics of DC immunobiology

Human DCs in the blood arise from the common myeloid progenitor cells originating from the bone marrow[21]. Normally, DCs patrol the peripheral tissues in an immature state. Upon encountering exogenous pathogens recognized by pattern recognition receptors (e.g. Toll-like receptors), immature DCs efficiently phagocytose the antigens, and promptly activate the maturation process. Mature DCs downregulate phagocytosis, increase secretion of pro-inflammatory cytokines (e.g. interleukin 12, IL-12), and upregulate expression of major histocompatibility complex (MHC) molecules (e.g. HLA-DR, an MHC class II molecule) and co-

stimulatory molecules (e.g. CD80, CD86 and CD40). Maturation is also associated with the upregulated expression of C-C chemokine receptor 7, which drives the homing of mature DCs into the draining lymph nodes[17,22,23].

Once in the draining lymph nodes, DCs engage the T-cell receptors (TCRs) and present the processed antigens to naïve T cells in complex with an MHC molecule. The interaction between antigen-MHC complex and TCR provides the antigen-specific "signal 1" needed for T cell activation. "Signal 2" involves complex cross-talk between pairs of counter co-stimulatory molecules present on the surface of DCs and T cells[24]. Upon receiving both signals from DCs, naïve T cells initiate programmes for proliferation and differentiation into antigen-specific effector T cells. $CD4^+$ T cells give rise to T helper cells, while $CD8^+$ T cells differentiate into effector cytotoxic T lymphocytes (CTLs)[22]. In the context of cancers, anti-tumor immunity is primarily mediated by $CD8^+$ CTLs, with $CD4^+$ T helper cells providing vital support to the proper functioning of $CD8^+$ CTLs. Effector $CD4^+$ and $CD8^+$ T cells localize to the tumor sites, where they eliminate tumor cells through cytotoxic activities and production of effector cytokines[24].

2.1.2 *Ex vivo* generation of clinical-grade Mo-DCs for cancer vaccine purposes

DCs constitute approximately 1% of naturally circulating leukocytes in human blood. Due to their low occurrence frequency in peripheral blood, DCs used for the manufacturing of cancer immunotherapies are commonly differentiated *ex vivo* from a progenitor cell source, normally $CD34^+$ hematopoietic progenitor cells or $CD14^+$ peripheral blood monocytes either from autologous (from the patients themselves) or allogeneic (from a donor) sources[22]. Differentiating autologous monocytes in the presence of IL-4 and granulocyte-macrophage colony-stimulating factor (GM-CSF) remains the most commonly used preparation method to generate clinical-grade DCs[18]. The differentiation phase usually lasts 5 to 7 days to generate immature Mo-DCs, followed by stimulation with a maturation cocktail for 48 hours to produce mature Mo-DCs[16]. Figure 2-1 details the differentiation and maturation protocol adopted by our team, which is developed by our collaborators at Dr. Michel L. Tremblay's lab.

Antigen loading represents the last but critical step to obtaining a functional Mo-DC-based cancer vaccine, as it specifies the target for the CTL-mediated anti-tumor immunity. This step can be done during or after the maturation phase by pulsing the *ex vivo* derived Mo-DCs with tumor-associated antigens (TAAs)[21]. Shared or defined TAAs were typically used in earlier trials to

generate broadly applicable cancer vaccines[21,22]. Recent advances in bioinformatics tools and RNA sequencing have made it possible to identify patient-specific neoantigens, which can be used as targets to manufacture personalized cancer vaccines that might exhibit improved clinical benefits[21,23]. The antigen-loaded Mo-DCs are then administered to patients, where they traffic to the draining lymph nodes to reengage the anti-tumor immunity mediated by $CD8^+$ CTLs. Figure 2-2 illustrates an overview of the manufacturing process of Mo-DC-based cancer vaccines.

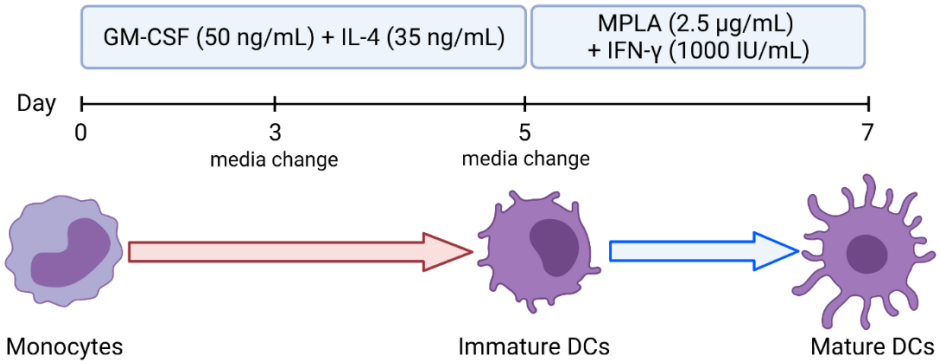

Figure 2-1 Mo-DC differentiation protocol adopted by our research group. Created with BioRender

2.1.3 Recent advances in Mo-DC cancer immunotherapy and future directions

The outcomes of a meta-analysis showed that following infusion of a DC-based vaccine, 77% of patients with prostate cancer and 61% of patients with renal cell carcinoma elicited immune responses[20,25]. In addition, patients receiving DC immunotherapy treatment had at least a 20% increase in median overall survival in almost all published trials where survival benefits have been studied[20]. In the phase III IMPACT study of the landmark sipuleucel-T, patients infused with sipuleucel-T showed a 4-month overall survival benefit versus patients treated with placebo[26].

Despite the proven immunogenicity and survival benefit of Mo-DC cancer immunotherapies, the overall clinical objective response rate remains poor[20,21]. As an example, < 5% of patients achieved an objective response in the IMPACT study of sipuleucel-T[20,26]. The clinical benefit is largely limited by the *in vivo* immunosuppressive microenvironment that *ex vivo*-derived Mo-DCs experience after infusion. To overcome this challenge, ongoing research efforts have been devoted to optimizing the differentiation and maturation protocols in order to generate Mo-DCs with enhanced immunostimulatory capacities. Another trend in optimizing the clinical performance of Mo-DC-based cancer vaccines is through combination therapy. Emerging data suggest that

harvesting the synergistic interactions between DC vaccination and other cancer treatments might be able to completely unleash the potential of DC-based immunotherapies[20,21].

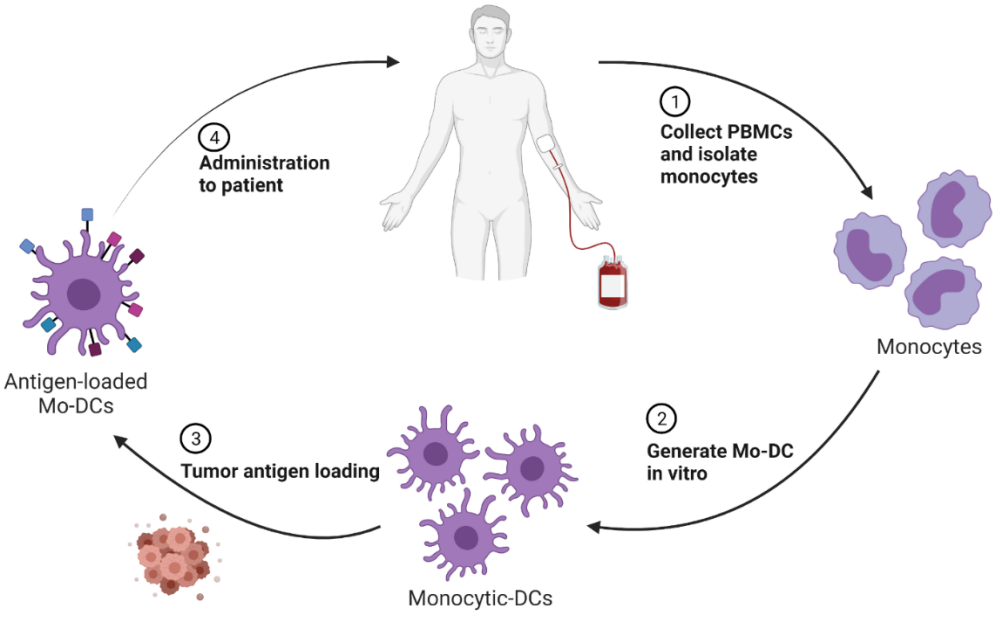

Figure 2-2 Overview of the manufacturing process of Mo-DC cancer vaccines. Created with BioRender

2.2 Moving towards cGMP-compliant manufacturing of Mo-DC immunotherapy

Aside from ongoing efforts from the immunological side to optimize the performance of *ex vivo*-derived Mo-DCs, important considerations from an engineering and manufacturing perspective have also gained much traction. The following section discusses current developments in strategically designed closed culture systems and specialized medium formulations that are tailored towards cGMP-compliant manufacturing of efficacious Mo-DC cancer immunotherapy.

2.2.1 Considerations of the culture medium: serum-free, chemically defined formulations

The standard medium formulation used in traditional Mo-DC culture protocols is the basal medium Roswell Park Memorial Institute (RPMI) 1640 supplemented with 10% heat-inactivated fetal bovine/calf serum (HI-FBS/FCS). FBS contains an abundance of components such as proteins and growth factors that are conducive to cell growth, albeit its ill-defined composition signifies a high batch-to-batch variability and inferior experiment reproducibility. Including FBS in the medium formulation also makes the culture more prone to contamination and transmission of harmful pathogens such as prions, viruses and mycoplasma[27,28]. Accordingly, manufacturers have developed medium formulations devoid of animal-derived serum which are preferred in clinical

applications. Although in most cases the composition of these serum-free media remains proprietary to the manufacturers, these formulations are generally thought to contain basal factors such as sugars, lipids, amino acids, hormones, vitamins, inorganic salts and a combination of proteins that are specifically designed for different cell types.

Table 2-1 Commercially available serum-free medium formulations optimized for Mo-DC culture

Company	Product Name	Classification
STEMCELL Technologies	ImmunoCult™-ACF Dendritic Cell Medium	serum-free, animal component-free
CellGenix	CellGenix® GMP Dendritic Cell Medium	serum-free, GMP-grade
PromoCell	Dendritic Cell Generation Medium XF	Serum-free, xeno-free
R&D systems	CellXVivo Human Monocyte-derived DC Differentiation Medium	Serum-free

Serum-free medium can be further classified into the following subgroups depending on the components present in the medium: xeno-free (does not contain non-human animal components but might contain human-sourced crude protein fractions such as human serum albumin), animal component-free (does not contain any animal-sourced components including from human), protein-free (entirely devoid of proteins or polypeptides) and chemically defined (does not contain any chemically undefined components such as crude protein fractions but could contain highly purified components such as recombinant proteins)[27]. Table 2-1 presents a number of serum-free Mo-DC medium formulations that are commercially available. Among them, ImmunoCult™-ACF Dendritic Cell Medium (STEMCELL Technologies) is a serum-free, animal component-free medium that contains only recombinant proteins and synthetic components. It is also the medium of choice in all experiments concerning monocytes/Mo-DC culture in the present project.

2.2.2 Considerations of the culture system: functionally-closed fluoropolymer culture bags

Polystyrene has been the most commonly used material for disposable lab wares for cell culture applications since the 1960s. Polystyrene itself is intrinsically hydrophobic, thereby providing limited interactions with adherent cell types. To facilitate cell adhesion and spreading, the polystyrene substrate is often functionalized, typically with a plasma treatment, to increase the surface hydrophilicity with the introduction of biologically relevant chemical groups (e.g. carboxyl

and amine groups)[29]. This surface-treated form of polystyrene is referred to as TCPS and is suitable for adherent or anchorage-dependent cell cultures.

Traditional polystyrene culture systems such as the T-flasks and multiwell plates have an open configuration. The vessels are opened and closed during manual manipulations, creating chances for contamination. By virtue of this reason, closed culture platforms such as fluoropolymer culture bags are preferred in the production of clinical cellular therapies as to minimize the risk of contamination, and comply with cGMP regulations. Fluoropolymers emerged as excellent substrates for cell culture because of their high-performance properties, such as mechanical flexibility, optical clarity, gas permeability, chemical resistance, thermal stability over a wide range of temperatures, and the ability to be melt-extruded or thermoformed[30,31]. FEP is one of the most commonly used fluoropolymers to manufacture commercially available culture bags; examples include the VueLife® C and AC series (Saint-Gobain) and PermaLife™ (OriGen Biomedical). The FEP culture bags are flexible, transparent, and gas (oxygen, nitrogen and carbon dioxide) permeable. In addition, the bags have the option to be connected to other cell culture processing units through aseptic tubings, which facilitate scale-up/scale-out and automation of cellular therapy production in a functional, fully closed bioreactor system[2]. A summary comparing the properties of fluoropolymer bags to polystyrene flasks is presented in Figure 2-3.

However, transitioning from polystyrene flask cultures to fluoropolymer bag cultures entails significant changes in the vessel substrate properties (e.g. surface chemistry, stiffness, topography), which could alter the culture microenvironment and affect the final cell fate decision of the cellular therapy products. The impact of culture vessel materials on *ex vivo*-derived Mo-DCs has been extensively studied by different research groups, as summarized in Table 2-2. Most authors reported no significant differences between Mo-DCs generated in bags versus flasks[3–5]. A few authors, on the other hand, reported a diminished secretion of IL-12 by bag-cultured Mo-DCs[6]. On our end, Mo-DCs cultured in FEP bags were observed to have comparable viability, phenotype, cytokine secretion profile and $CD8^+$ T cell stimulatory capacity as compared to those cultured in TCPS flasks[5]. In addition, we and others observed heterogeneity in Mo-DCs cultured in FEP bags classified by their adherence characteristics (i.e. a fraction of monocytes and/or Mo-DCs adhered to FEP surfaces instead of completely remaining in suspension)[5,6]. In fact, some groups harvested only the non-adherent fraction as qualified Mo-DCs and regarded the adherent fraction as

macrophage-like cells[4,32,33]. Conversely, other groups documented that adherent Mo-DCs were functionally equivalent or even superior to the non-adherent cells[34,35]. Furthermore, some traditional protocols rely on the plastic adherence of monocytes and/or Mo-DCs[36,37], whereas more recent research efforts have demonstrated that the generation of mature Mo-DCs could completely be carried out in suspension cultures[2,5,38]. All of these disparities lead to a still-unsolved question: Is plastic adherence necessary for the efficient culture of a facultative adherent cell type such as monocytes/Mo-DCs? As of now, it is still impossible to reach a consensus on whether the selection of different culture materials impacts the adhesion behavior and the resulting phenotypical and functional properties of Mo-DCs[2]. More systematic studies and strategically designed potency assays are indeed necessary to resolve the puzzle.

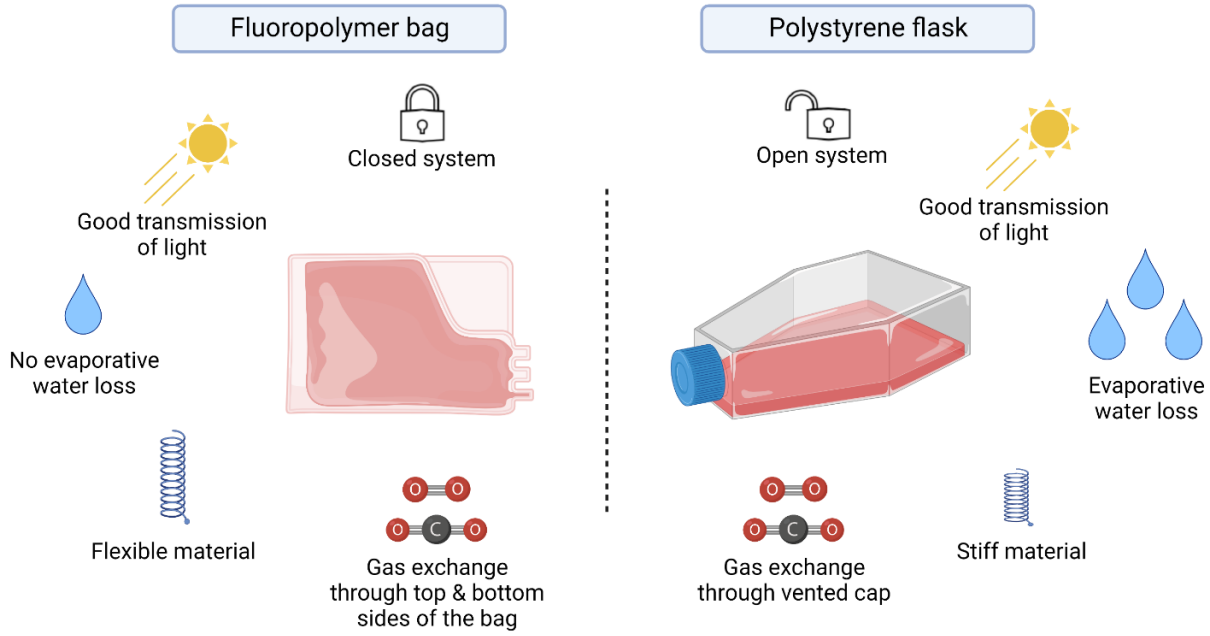

Figure 2-3 Comparison of physical properties of fluoropolymer bags vs. polystyrene flasks. Reproduced from Fekete et al.[2]. Created with BioRender

Furthermore, the mechanisms by which monocytes/Mo-DCs adhere to fluoropolymers are poorly characterized. Identifying the cell adhesion mediators will pave the way for us to study the mechanotransduction and downstream signaling pathways that are triggered during the adhesion process, which will help us answer the question of whether cell adhesion is beneficial for Mo-DC culture. Of note, understanding the adhesion mechanisms will as well provide us with critical insights into how to better engineer the culture materials towards promoting or inhibiting cell-surface adhesion depending on whether plastic adherence is beneficial for Mo-DC maturation.

Table 2-2 Studies comparing Mo-DCs cultured in bags vs. flasks. Adapted from Fekete et al.[2]

Reference	Bag		Flask	Potency assays	Major outcomes
Bastien, 2020[5]	FEP	vs.	TCPS	FC, ELISA, viral antigen presentation	No statistically significant differences observed in viability, yield, phenotype, cytokine levels (IL-6, IL-12, IL-10) and antigen-specific T cell stimulation.
Kurlander, 2006[6]	FEP	vs.	Polystyrene	FC, ELISA, DC migration assay, IFN-γ production by autologous T cells	DCs were comparable in yield, viability, phenotype, antigen-specific T cell stimulation but produced significantly less IL-12 & IL-10, and displayed slightly enhanced migration in FEP.
Wong, 2002[3]	FEP	vs.	Polystyrene	FC, MLR, autologous recall responses to tetanus toxoid and influenza virus	DCs were equivalent in yield, phenotype and *in vitro* function.
Suen, 2001[4]	FEP	vs.	TCPS	FC, MLR, dextran uptake (pinocytosis)	DCs has similar viability, yield, purity, phenotype and function.

FC: flow cytometry, ELISA: enzyme-linked immunosorbent assay, MLR: mixed lymphocyte reaction

2.3 Plasma surface modification: an efficient strategy to functionalize polymeric biomaterials

Synthetic polymers such as polystyrene and fluoropolymers have been broadly used in biological applications including *in vitro* cell culture owing to their excellent bulk properties such as mechanical strength, chemical resistance and biocompatibility[39,40]. However, many polymeric substrates have intrinsically low surface energy, which largely limits their interactions with bio-macromolecules and cells[41]. A common approach to tackle this limitation is to apply a surface modification treatment to the polymer substrate, which renders the substrate surface more hydrophilic without affecting the favorable bulk properties. Plasma surface treatment is considered

a prominent strategy due to its high reproducibility, versatility, minimal waste production and solvent-free nature[39,40].

2.3.1 Plasma generation and classification

Plasma is often referred to as the fourth state of matter[40,42]. When gas molecules are provided with sufficient energy, some or all molecules will have gained enough energy to ionize, resulting in a mixture of ions, free electrons, radicals, photons, and neutral species that is so-called a plasma. Plasma is generally classified into two main categories: thermal and non-thermal plasmas, depending on the gas temperature at which the process is operated[40]. For the surface treatment of polymeric substrates, non-thermal low-temperature plasma is mostly used as it does not impose thermal damage to the polymers. There exist multiple methods for supplying the ionization energy source to excite the plasma, but applying an electrical potential remains the most commonly used strategy to generate non-thermal gaseous plasma, which is generally referred to as electrical discharge plasma[43,44].

Electrical discharge processes come in two basic types: low-pressure (or vacuum) and atmospheric discharge[43]. Low-pressure plasma systems employ a vacuum chamber whereby ambient gas in the chamber is pumped out and then filled with the desired process gas at a pre-set and controlled pressure. Atmospheric plasma, by name, operates at atmospheric pressure and does not require additional apparatus such as a vacuum chamber and vacuum pump. Corona discharge in air is perhaps the best example of atmospheric plasmas, and is widely used in the treatment of TCPS cultureware by several manufacturers, including Nunclon Delta® (Thermo Scientific) and CellBIND® (Corning). It is generated by applying a high voltage to an electrode in the form of a wire or a sharp tip[42,45]. As air or surrounding gas passes through the electrode, a fraction of the gas molecules are ionized, leading to the formation of a corona discharge. Despite the simplicity and lower cost of atmospheric corona discharge, they provide inferior control over the physicochemical characteristics of the treatment modalities in comparison to low-pressure plasma treatments. Therefore, there has been a growing trend towards using low-pressure plasma to generate highly functional, finely tuned surface treatments for *in vitro* cell culture applications.

2.3.2 Plasma polymerized coatings

There exist different interaction modes between a plasma and a surface which gives rise to various plasma modification techniques including plasma polymerization, plasma-induced grafting (of

chemical functionalities), plasma activation, sputtering and etching, and plasma syn-irradiation. The underlying principles and reaction mechanisms of these different techniques have been extensively reviewed elsewhere[39,40]. In the framework of this thesis, we will focus on introducing the plasma polymerization technique.

Plasma polymerization employs a polymerizable monomer in either gas or liquid state at the plasma discharge, which gets converted into reactive fragments that form a highly cross-linked plasma polymer coating (PPC) upon reacting with a surface[40]. Hydrocarbons are frequently used as the monomer of choice, but a wide range of monomers can be plasma polymerized, including methane which is non-polymerizable by classical means. Considering the important roles of oxygen- and nitrogen-containing functional groups in the context of biological applications, one or more heteroatom gas sources rich in oxygen or nitrogen elements (e.g. carbon dioxide and ammonia) are often mixed with a polymerizable hydrocarbon gas (e.g. ethylene and butadiene) to form the precursor gas mixture. The resulting active species condense onto the substrate, forming an organic thin-film coating with oxygen- and/or nitrogen-containing functionalities implanted in the cross-linked hydrocarbon backbone. The concentration of implanted functional groups can be controlled by adjusting the deposition process parameters such as the hydrocarbon-to-heteroatom gas ratio. A set of oxygen-rich and nitrogen-rich PPCs have been developed and characterized by different research groups to study their potentials in biological and biomedical applications[14,41,43,46].

2.3.3 Development of gradient plasma polymer coatings rich in oxygen- and nitrogen-containing functionalities

PPCs naturally undergo “aging” over storage time, leading to the so-called hydrophobic recovery of the surface[47]. The aging phenomenon is driven by the reorientation and migration/diffusion of the plasma-induced surface functionalities to minimize the surface free energy and to return to an equilibrium state. Other reactions such as oxidation and hydrolysis are also involved in this process, especially upon steam sterilization or immersion of the PPCs in an aqueous environment[47,48]. In particular, N-rich PPCs often suffer from rapid aging and low stability due to the reactivity of nitrogen functional groups (such as amines and imines) with oxygen and water molecules.

The stability of the PPCs can be enhanced by elevating the degree of cross-linking at the near-surface layer, which limits the freedom of reorientation of functional groups in the polymer bulk and hinders water intrusion during steam sterilization and/or cell culture[48,49]. However, this

increase in stability is offset by an undesired reduction in surface hydrophilization associated with the lower density of functional groups in more cross-linked PPCs. In addition, enhanced cross-linking affects the mechanical properties of the PPCs (e.g. increased stiffness) which might become unfavorable for cell interactions[49]. To circumvent this challenge, a few authors have explored a recently emerging trend to obtain stabilized but functional PPCs, which constitutes preparing a vertical chemical gradient with a highly functional (less cross-linked) layer at the uppermost surface and a highly cross-linked layer towards the inside[48,49]. Gradient plasma polymer coatings (GPPCs) deposited using this strategy have been proven to experience a much-reduced aging process[48,49].

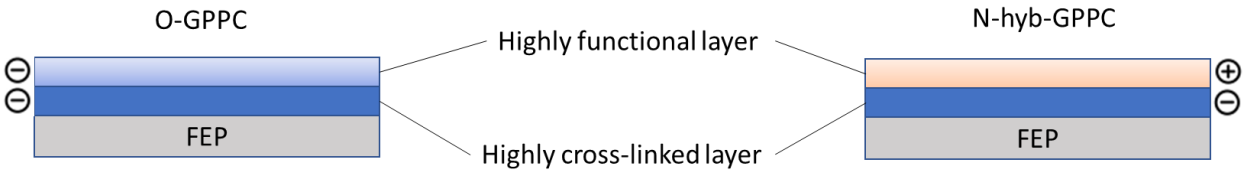

Figure 2-4 Schematic of the GPPC configuration

To explore the concept of GPPCs further, our team previously developed oxygen-rich GPPC (termed O-GPPC) with a low-pressure capacitively-coupled PECVD reactor[1]. The coating consists of a highly cross-linked base layer and a highly functional surface layer with a vertical gradient, as illustrated in Figure 2-4. The vertical gradient is achieved by varying the hydrocarbon-to-heteroatom gas ratio as opposed to varying the power by other authors, which results in improved homogeneity of the coating. We also developed GPPCs rich in nitrogen functionalities. Considering the inferior stability of N-containing PPCs in general, we introduced a hybrid (containing both O and N elements) highly cross-linked layer that is oppositely charged to the highly functional layer. The electrostatic attraction between the two layers is expected to further improve the stability. This coating is thus named nitrogen-rich-hybrid GPPC (N-hyb-GPPC).

The GPPCs were designed to be compatible with an extended storage time when compared with regular PPCs. In unpublished data (currently awaiting patent application filing)[1], we have demonstrated the stability of O-GPPC and N-hyb-GPPC post sterilization, as assessed by surface characterization techniques including X-ray photoelectron spectroscopy (XPS), profilometry and water contact angle analysis (Figure 2-5). No thickness loss was observed and only minimal hydrophobic recovery was seen after steam sterilization (121 °C and 15 psig for 15 min). However,

to our knowledge, the potential of GPPCs in cell culture applications has never been investigated, which is one of the main focuses of this thesis work.

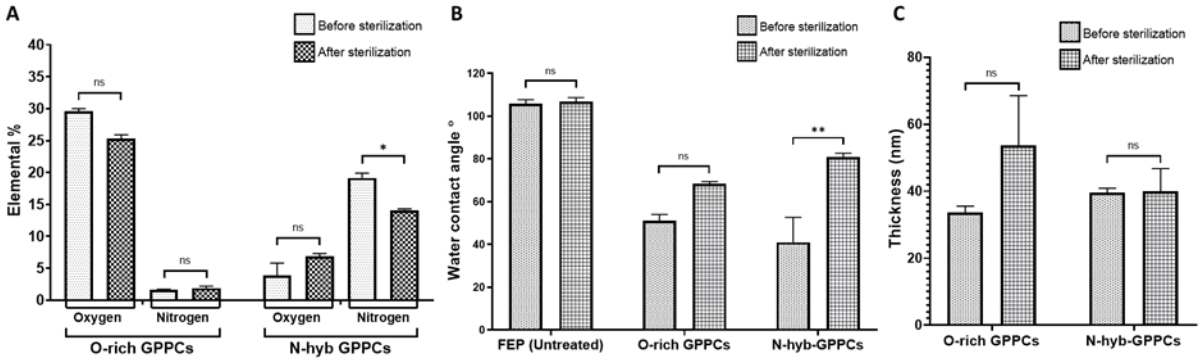

Figure 2-5 Surface characterization of O-GPPC & N-hyb-GPPC before and after sterilization. (A) Percentage of oxygen and nitrogen. (B) Water contact angle measured using a goniometer. (C) Thickness measured using profilometry. Unpublished data from Ramachandran et al.[1]

2.4 Mechanisms of monocyte adhesion to culture substrates

In the context of cell culture in a protein-containing medium, it has been widely thought that cell-surface interactions are in fact between cells and surface-adsorbed proteins rather than directly between cells and surfaces themselves. Upon contact with the culture vessel, proteins derived from the culture medium instantly adsorb onto the surface and form a protein adlayer covering the base substrate. This phenomenon happens within a much shorter timeframe than cells can migrate to the interface. Therefore, cellular attachment to the culture substrate is proposed to proceed through the binding of cell surface adhesion molecules, particularly integrin receptors, to adhesive protein ligands that are adsorbed on the substrate surface[7].

2.4.1 Impact of surface properties on cell behavior at the substrate interface

Substrate physiochemical properties such as surface charge, chemical makeup and hydrophilicity impose determining effects on the protein adsorption phenomenon at the substrate interface. The type, amount and conformation of proteins constituting the protein adlayer in turn control the behavior of cells when they come into contact with the surface. In general, protein adsorption onto a solid surface is governed by the net surface charge and interfacial free energy between the surface and the aqueous medium atop[10]. Some authors described a competition between adhesion-inhibiting globular proteins (such as albumin) and large pro-adhesion proteins (such as fibronectin) for adsorption onto solid surfaces. Hydrophilic substrates with high surface free energy (lower interfacial free energy) were observed to favor the adsorption of pro-adhesion proteins, whilst

hydrophobic surfaces were found to have a higher amount of surface-adsorbed albumin[10,11]. Correspondingly, Zelzer *et al.* demonstrated that hydrophilic substrates with a higher amount of surface-adsorbed fibronectin significantly enhanced adhesion and proliferation of fibroblasts as opposed to the hydrophobic controls[11].

Numerous studies have been conducted to investigate the effects of surface modification by plasma polymerization on the propensity of cells to adhere. For example, it has been reviewed elsewhere that the introduction of biologically relevant functionalities such as primary amines (-NH_2), hydroxyl (-OH), and carboxyl (-COOH) groups led to enhanced adhesion of various cell types[11,12,50]. Past studies by our team revealed that the number of adherent monocytes correlated to the concentration of functional groups present on the surface[14]. In addition, a critical threshold concentration of functional groups at the substrate surface ([NH_2]=2.6-3.0%, [COOH]=1.2-1.57nmol/cm^2) was identified, above which the adhesion of a typically non-adherent cell type, U937, was facilitated[14]. These studies reveal that material surface properties play decisive roles in controlling cell behavior at the substrate interface, which presents a prospect to potentially modulate cell-surface interactions by tuning the substrate surface chemistry with plasma surface treatment techniques.

2.4.2 Lessons learned from previous studies on TCPS

In unpublished data, our team previously demonstrated that 40±25% of Mo-DCs adhered to untreated FEP following a 9-day culture through a mechanism that was unclear[51] (Figure 2-6). Previous studies on monocyte adhesion mechanisms have mostly been conducted on polystyrene-based surfaces. Key findings of various studies are summarized in Table 2-3 below. To determine whether cell adhesion is mediated by integrins, many of these studies have employed ethylenediaminetetraacetic acid (EDTA), a chelator that is well-known for inhibiting integrin-mediated adhesion by binding to divalent cations including Ca^{2+}, Mg^{2+} and Mn^{2+} in such a way that these cations are prevented from coordinating integrin ligation. Various authors reported a complete or nearly complete adhesion inhibition at EDTA concentrations varying from 2 to 10 mM[52–54]. Interestingly, Shen *et al.* reported that the addition of EDTA after monocytes were allowed to adhere for a certain period of time could only partially interfere with cell adhesion, as opposed to its ability to completely inhibit monocyte adhesion if added prior to seeding[52].

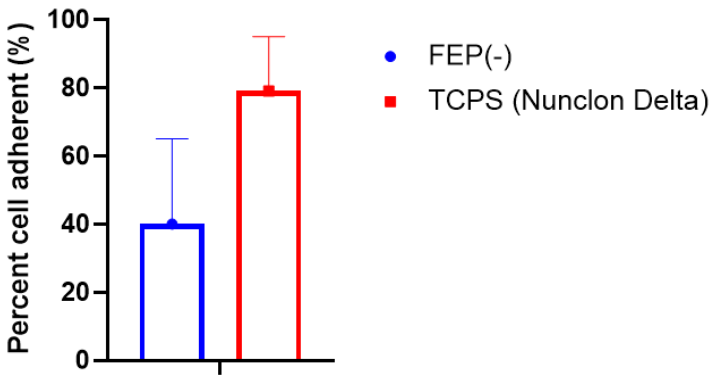

Figure 2-6 Frequency of adherent Mo-DCs on untreated FEP and Nuclon Delta-treated TCPS. Previously unpublished data from Fekete et al.[51]

Many studies also employed anti-integrin monoclonal antibodies to address the specific identities of integrins that are implicated in monocyte adhesion to polystyrene-based surfaces. It has been suggested by numerous authors that the β2 integrin subfamily consisted of the major monocyte-surface adhesion mediators[52–57]. Blocking of the β2 subunit in most studies exhibited a significant inhibitory effect[53,54,56], whereas blocking of the α subunits (αX, αM, αL) in some studies imposed only limited or minimal adhesion inhibition[55,57]. In addition, despite the proposed crucial role of β2 integrins, some studies conducted by blocking the β2 integrins exhibited only partial inhibition of monocyte adherence, indicating that β2-independent adhesion mechanisms might occur with polystyrene-based surfaces[55].

On the other hand, whether the Arg-Gly-Asp (RGD)-binding integrins (α4β1, α5β1 and αVβ3) contribute to mediating monocyte initial adhesion remains ambiguous. McNally and Anderson[53] added fibronectin fragments containing the RGD motif to their culture, but observed no disruption in monocyte adhesion. In addition, immunofluorescence studies revealed that these integrins weren't even expressed by their monocyte populations. On the other hand, Orgovan *et al.* observed heightened monocyte initial adhesion on surfaces pre-coated with a synthetic RGD-containing copolymer[58]. Some other studies also confirmed the expression of these RGD-binding integrins on human monocytes, and suggested that they were potentially involved in monocyte-surface interactions[59,60]. Furthermore, electrostatic effects might also play a role in cell-surface interactions, as reviewed by Wertheimer *et al.*[61] and Hoshiba *et al.*[62].

Table 2-3 Key findings of previous studies on monocyte adhesion mechanisms to culture substrates

Author, Year	Cell type	Surface	Results
Babaei *et al.*, 2018[14]	U937, NB4, monocytes	N- and O-rich PPCs	1. The O- and N-rich organic coatings promoted cell adhesion, but only if the coatings contain a minimum functional group content. 2. The number of adherent monocytes was proportional to functional group composition (COOH, NH_2) in the coatings. 3. Podosomes were observed on nearly all surfaces that promoted cell adhesion. 4. Presence of albumin on the PPC-coated surfaces above the defined critical concentration might indicate the adhesion of monocytes to the PPCs. 5. Main conclusion: Modifying the nitrogen content in the PPCs could turn a surface from adhesion-deterrent to adhesion-promoting for specific cell types; a phenomenon that could be exploited to select certain cell types from a mixture by exposing the mixture to a PPC containing a particular nitrogen content.
Sándor *et al.*, 2016[57]	Monocytes, Mo-DCs	TCPS coated with fibrinogen	1. Blocking αX resulted in a partial (~20%) reduction in monocyte adhesion. Blocking αM had no significant effect. 2. Blocking αM significantly decreased monocyte adhesion strength. 3. Main conclusion: αXβ2 dominates adhesion of monocytes to fibrinogen over αMβ2.

McNally and Anderson., 2002[53]	Monocytes	RGD-modified (Pronectin F-coated) TCPS well plate	1. EDTA and EGTA at 10mM either completely or nearly completely inhibited initial monocyte adhesion. 2. Addition of RGD peptides in the media had no impact on initial monocyte adhesion. 3. Anti-β1 antibodies (clone JB1a & 6S6) and anti-β3 antibody (clone B3A) did not impact initial monocyte adhesion, whereas anti-β2 antibodies (clone YFC118.3 & MHM23) either partially or completely inhibited monocyte adhesion. 4. Main conclusion: Initial monocyte adhesion is likely mediated by β2 integrins, and independent of pathways binding to RGD-containing proteins.
Shen *et al.,* 2001[52]	Monocytes	4 polystyrene-based surfaces (PS, TCPS, Primaria, ULA), pre-incubated with 1% plasma	1. Monocyte adhesion linearly and positively correlated with the amount of fibrinogen adsorbed on each tested surface. 2. Addition of EDTA before seeding the cells reduced monocyte adhesion in a dose-dependent manner. Monocyte adhesion was completely inhibited at 2mM EDTA. 3. Addition of EDTA after the cells started to adhere only partially reduced adhesion and cannot completely inhibit adhesion even at high EDTA concentrations. 4. Main conclusion: Initial monocyte adhesion to polystyrene-based surfaces is mediated by fibrinogen-binding integrins, possibly αMβ2; initial adhesion has an important effect on long-term adhesion.
Garnotel *et* al., 2000[54]	Monocytes	TCPS coated with acid-soluble or pepsin-digested collagen I	1. Adhesion was reduced by 85% with 5 mM EDTA. 2. Antibodies against αX (clone FK-24 and 5-HCl-3) and β2 (clone MEM-48 and MHM-23) significantly reduced monocyte adhesion. 3. Slight but significant adhesion reduction was observed by blocking β1 (with clone P4C10). 4. No significant inhibition was observed by blocking αL and αM. 5. Main conclusion: monocytes interact with type I collagen through αXβ2.

Patarroyo *et* al., 1998[55]	Monocytes	TCPS	1. Blocking of the β2 subunit alone with mAbs 60.3 showed an inhibitory effect. 2. Blocking of the α subunits, αX (with Anti-Leu-M5), αM (with 60.1), and αL (Anti-LFA-1) individually showed either limited or minimal inhibitory effects, but combination of the three showed inhibitory effect that was comparable to blocking of β2 with 60.3. 3. Main conclusion: β2 integrin, either alone or associate with αX, αM, or αL mediates monocyte adhesion. However, blocking of β2 did not exhibit full inhibition of monocyte adhesion to plastics, indicating the existence of β2-independent adhesion mechanisms.
McNally and Anderson., 1994[56]	Monocytes	Modified polystyrene-based surfaces (fluorinated, siliconized, nitrogenated, oxygenated)	1. Blocking of β2 integrins (60.3, MHM23) inhibited initial monocyte adhesion to all four tested surfaces. Blocking of αM (60.1) also exhibited a partial inhibitory effect. 2. Adhesion to surfaces reduced by 50-100% when complement component C3-depleted serum was used, but restored when C3 was replenished, indicating interactions between C3 and αM/β2 promote monocyte adhesion. 3. Adsorbed fibrinogen reduced effectiveness of mAbs tested. 4. Main conclusion: Alternate adhesion pathways may be adopted depending on the propensities of adhesion-mediating components present on different surfaces.

2.5 Integrins: the primary cell-surface interaction mediators

Integrins along with selectins, cadherins and members of the immunoglobulin superfamily (IgSF) make up the four major groups of CAMs. Typically, selectins, cadherins and IgSF members are cell-cell adhesion mediating molecules, while integrins are identified as the major receptors for ECM proteins, which facilitate cell-surface interactions[8,9]. Integrins are heterodimeric adhesion receptors that are formed through the non-covalent association of two type I transmembrane glycoproteins, termed the α- and the β-subunit[63]. 18 α- and 8 β-subunits are currently identified in

vertebrates, which associate to form 24 functional heterodimers, each having a distinct ligand binding profile and affinity[64].

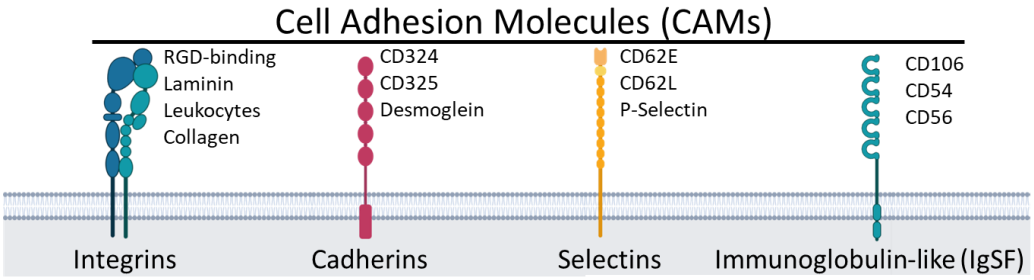

Figure 2-7 Classification of cell adhesion molecules.Created with BioRender

2.5.1 Integrin system expressed by monocytes

Human peripheral blood monocytes have been characterized for the expression of eight integrin heterodimers: α1β1, α3β1, α4β1, α5β1, αLβ2, αMβ2, αXβ2 and αVβ3[60]. Table 2-4 outlines the commonly recognized ligands and reported expression levels for each of these eight integrins. To be noted, a ninth integrin, αDβ2 (CD18/CD11d), was shown to express on circulating monocytes in recent years[65], but the ligand-binding specificity of this integrin is not yet well-understood.

Table 2-4 Integrin system expressed by monocytes

β subunit	α subunit	Common ligands	Reported expression level
β1 (CD29)	α1 (CD49a)	• Laminin, collagen • Recognize G-F-P-G-E-R sequence in collagen	• Low expression: MFI ratio to isotype control (35:8)[66]
	α3 (CD49c)	• Fibronectin, laminin, collagen, epiligrin etc. • Recognize R-G-D sequence	• Low expression: MFI ratio to isotype control (14:8)[66]
	α4 (CD49d)	• Fibronectin by recognizing domains in CS-1, CS-5 regions • VCAM-1	• Low expression: MFI ratio to isotype control (19:8)[66]
	α5 (CD49e)	• Fibronectin & fibrinogen • Recognize R-G-D sequence	• Mid-low expression: MFI ratio to isotype control (70:8)[66]
β2 (CD18)	αL (CD11a)	• ICAM 1-4	• High expression: MFI ratio to isotype control (180:8)[66] • High expression: MFI ratio to isotype control (230:50)[65] • High expression[67]

	αM (CD11b)	• More than 40 dissimilar ligands • Complements iC3b, C4b • fibrinogen • ICAMs	• High expression, MFI ratio to isotype control (155:8)[66] • Mid-high expression, MFI ratio to isotype control (120:50), similar to CD14[65] • High expression[67] • Ratio of CD11b/CD11c: 7.1; CD11b& CD11c competes for binding to fibrinogen[57]
	αX (CD11c)	• Similar binding specificity as CD11b due to sequence similarity (e.g. iC3b, ICAM-1) • Fibrinogen by binding G-P-R	• Mid-low expression: MFI ratio to isotype control (53:8)[66] • Mid-high expression: MFI ratio to isotype control (120:50), similar to CD14[65] • High expression but relatively lower than CD11a & CD11b[67]
	αD (CD11d)	• ICAM-3, VCAM-1 • Newly discovered, proposed to bind to fibronectin, fibrinogen, vitronectin like CD11b.	• Mid-high expression: MFI ratio to isotype control (150:50), similar to CD14[65] • High expression but relatively lower than CD11a & CD11b[67]
β3 (CD61)	αV (CD51)	• Vitronectin, fibronectin, laminin, collagen. • Recognize R-G-D sequence	• High expression of β3 subunit; Both β3 and αV upregulated upon adhesion to type I collagen & fibronectin[60]

2.5.2 Basics of integrin structure

Members of the integrin family adopt a shape of a "head" supported by two rod-like "legs", and reveal three structural components: the ectodomain (the extracellular domain), the transmembrane helices, and the cytoplasmic tails[64,68]. Figure 2-8 illustrates the integrin αXβ2 in both the bent (inactive) and upright (activated) conformations. The α-I domain and the β-propeller of the α-subunit together with the β-I-like domain of the β-subunit form the globular head region where ligand binding to integrins occurs. In those integrins that contain an α-I domain, ligand binding occurs predominantly at the metal-ion-dependent adhesion sites (MIDAS), where ligation is mediated through coordination to a Mg^{2+} ion. In α-I-less integrins, ligand binding occurs at the interface between the β-propeller and β-I-like domain. At the interface, there exist metal-ion-

binding motifs that are structurally similar to the MIDAS, as well as various other cation binding sites that recruit Ca^{2+} and Mn^{2+} ions to regulate the ligand binding affinity[64].

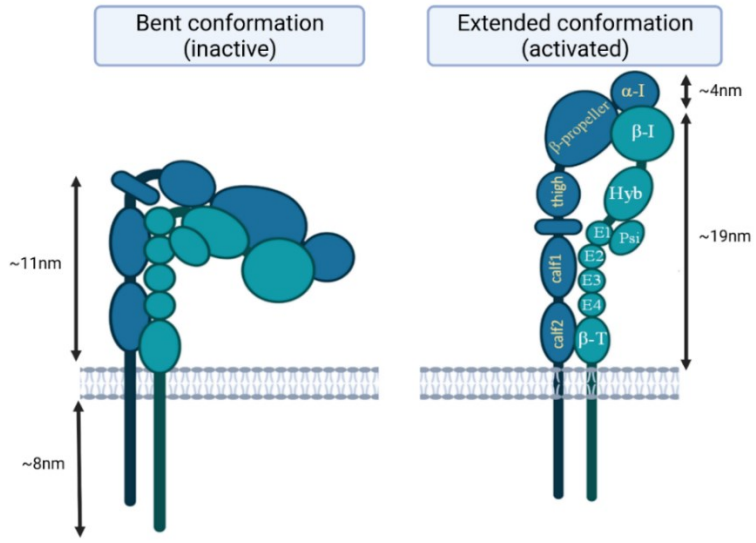

Figure 2-8 Graphical representation of αXβ2 in bent and upright conformations. Created with BioRender

2.5.3 Ligand binding mechanisms of integrins

Based on the nature of the molecular interactions, the mechanisms of integrin-ligand binding can be categorized into four main classes. The RGD-binding integrins, including all five αV integrins, α5β1, α8β1 and αIIbβ3, recognize ligands that contain the RGD motif[64]. The binding was determined to take place at the interface between the β-propeller and the β-I-like domain[64,69]. The integrins α4β1, α4β7 and α9β1 bind to a motif termed "LDV", which is an acidic motif that is functionally related to RGD. Similar to RGD, LDV peptide also binds to integrins at the β-propeller/β-I-like-domain junction. Ligands that bind to β2 integrins contain motifs that are structurally homologous to the LDV peptide, but the binding occurs at the α-I domain instead of the β-I-like-domain[64]. The integrins α1, α2, α10 and α11 associate with the β1 subunit in forming a distinct subfamily of integrins that binds laminin and collagen. In addition, three receptors of the β1 subfamily (α3, α6 and α7) bind selectively to laminin[64].

It is worth noting that β2 integrins are the predominant integrin receptors on leukocytes, and as previously mentioned, human monocytes express all four members of the β2 integrin subfamily. Speaking of the main ligands for the β2 integrins, briefly, αLβ2 mediates primarily cell-cell adhesion and binds to ICAM receptors on other cells. αMβ2 has a rather broad ligand binding profile that consists of over 40 ligands, including fibrinogen and fibronectin. Due to sequence

similarities, αXβ2 has a similar but more restricted ligand repertoire compared to αMβ2. Ligands for αDβ2 have not yet been extensively characterized, but have been proposed to overlap to large extent with those of αMβ2[8,67,70].

2.5.4 Integrin-containing cell-matrix adhesome structures

Typically, the mechanical force exerted on cells upon binding of integrins to the ECM triggers the assembly of cell-matrix adhesions. This process is generally believed to initiate with the physical clustering of integrins and ligands across the cytoplasmic membrane, followed by the recruitment of cytoskeletal adaptor proteins (such as talin, α-actinin and vinculin) and signaling molecules sequentially to the interface[9,71]. Based on morphological characteristics and molecular compositions, cell-matrix adhesions are typically classified into focal complexes, focal adhesions, fibrillar adhesions and podosomes (Table 2-5). Focal complexes are the first adhesions to be formed upon cell contact with the ECM, hence they are often termed the "nascent cell-matrix adhesions". They adopt a small, dot-like shape and are mainly present at the edges of the lamellipodium[71]. These structures might be transient or they may mature into focal adhesions at exposure to tension. Focal adhesions are the earliest- and best-characterized adhesion structures. Compared to focal complexes, they have a large, flat, elongated structure and are often located close to the periphery of cells[9,63]. Fibrillar adhesions associate with ECM fibrils and are usually located in the central regions of cells. Finally, podosomes are small, highly dynamic adhesion structures which adopt a cylindrical shape of an actin-rich core surrounded by a ring complex comprising integrins and typical focal contact proteins such as vinculin and paxillin.

Table 2-5 Morphological and compositional differences between different types of cell-matrix adhesomes

	Focal complexes	**Focal adhesions**	**Fibrillar adhesions**	**Podosomes**
Location	lamellipodium edge	cell periphery	cell central region	ventral surface of cells
Morphology	small, dot-like	flat, elongated	fibrillar or beaded	cylindrical with an actin core and an integrin-containing ring
Size	1 μm	2-5 μm	1-10 μm	0.5-2 μm
Typical compositions	paxillin, vinculin, phosphotyrosine	paxillin, vinculin, talin, focal adhesion kinase	tensin	talin, vinculin, paxillin, Src family proteins

3 MATERIALS AND METHODS

3.1 Deposition of gradient plasma polymer coatings on FEP substrates

O-GPPC and N-hyb-GPPC were deposited onto FEP films using our in-house-built, low-pressure, capacitively-coupled PECVD reactor following well-established protocols developed by Girard-Lauriault *et al.*[41,43,72]. The PECVD reactor is comprised of a cylindrical stainless steel vacuum chamber surrounded by a glovebox containing an inert atmosphere (oxygen content < 0.1ppm). Within the chamber, a disc-shaped electrode on which samples are placed is connected to an automatic impedance matching network that generates a capacitively-coupled radio frequency (RF) power discharge. A showerhead distributor is mounted face-to-face 4cm above the powered electrode, through which gas mixtures containing ethylene (as the hydrocarbon source), and carbon dioxide or ammonia (as the heteroatom source) were introduced into the reactor chamber. The chamber is purged using a combination of rotary vane and turbomolecular pump to create a high vacuum. Figure 3-1 depicts the physical configuration and schematic view of the PECVD reactor.

Table 3-1 Deposition parameters for O-GPPCs & N-hyb-GPPCs

Sample	Steps	Deposition	RF power	Pressure	Treatment time	Gas flow rate (sccm)		
						C_2H_4	NH_3	CO_2
O-GPPCs	1	NH_3 pre-treatment	60 W	13.3 Pa	45 s	0	15	0
	2	O-rich crosslinked layer	20 W	80 Pa	5 min	5	0	40
	3	O-rich functional layer	20 W	80 Pa	90 s	5 to 2.5	0	40
N-hyb-GPPCs	1	NH_3 pre-treatment	60 W	13.3 Pa	45 s	0	15	0
	2	O-rich crosslinked layer	20 W	80 Pa	3 min	20	5	20
	3	N-rich functional layer	20 W	80 Pa	90 s	20 to 10	0	15

Unmodified FEP films (Saint-Gobain, referred to as FEP(-)) were cut to sizes of 5.5cm x 2.5cm, cleaned with 70% ethanol in an ultrasonic bath, rinsed with reverse osmosis (RO) water, and vacuum-dried overnight. Clean FEP films were then loaded into the vacuum chamber and placed on the RF-powered electrode. The treatment parameters (Table 3-1), including chamber pressure, treatment duration, gas mixture compositions and flowrates were controlled by the users with a LabVIEW® program connected to the mass flow controllers and the RF power generator. FEP was first pre-treated with ammonia to enhance its cohesion with the overhead plasma polymer layers.

Next off, a highly crosslinked, oxygen-rich layer was deposited following the ammonia pre-treatment. Finally, a highly functional layer containing a vertical gradient of O-rich or N-rich functional groups was deposited as the uppermost surface layer of the coating. This chemical gradient was achieved by varying the flowrate ratio of ethylene to carbon dioxide (or ammonia), which is the key parameter that controls the density of functional groups in plasma-generated polymers. After the deposition, samples were sealed in oxygen-barrier bags (0.001 cc/m^2/day) and preserved at -40 °C in an inert atmosphere until use in cell cultures.

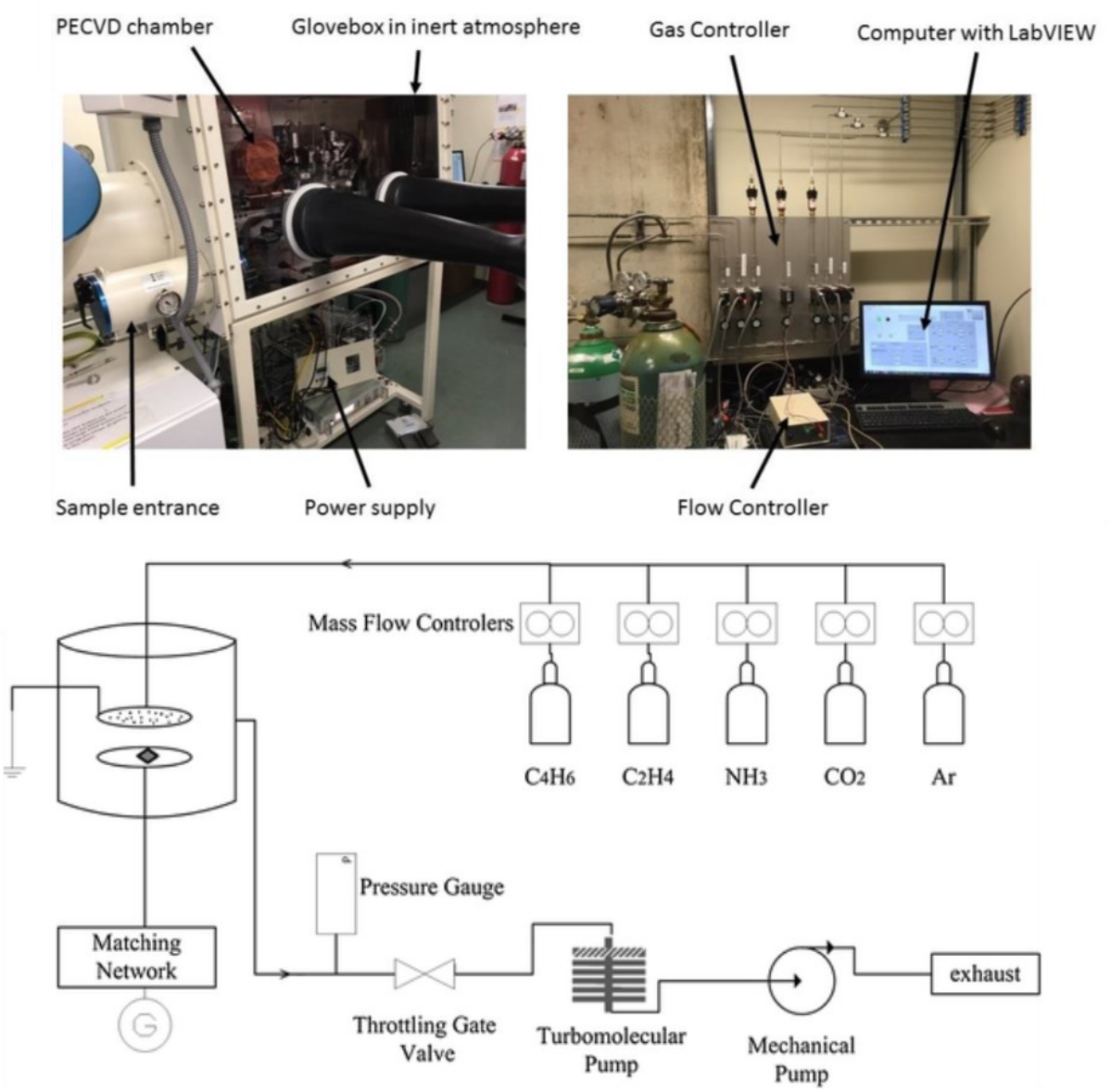

Figure 3-1 Physical configuration and schematic view of the PECVD reactor

3.2 Isolation of monocytes from human peripheral whole blood

3.2.1 Ficoll density gradient centrifugation

Fresh whole blood was collected from healthy volunteer donors after informed consent under the ethical guidelines approved by the McGill Institutional Review Board (Study Number: A06-M33-15A). 120 mL of whole blood was collected from each donor in heparin-coated vacutainers (BD, Cat. 367874) at the McGill University Health Centre and transported to the Stem Cell Bioprocessing Laboratory for subsequent processing. Blood was first diluted at a 1:1 ratio in Dulbecco's phosphate-buffered saline (DPBS, ThermoFisher, Cat. 14190144) supplemented with 2% human serum albumin (HSA, Sartorius, Cat. 05-730-1E). Diluted blood was then gently layered on top of Histopaque®-1077 (Sigma, Cat. 10771) in SepMate™-50 tubes (STEMCELL™ Technologies, Cat. 85450) and exposed to density gradient centrifugation at 1200 x g. The centrifuged blood was composed of multiple layers. The buffy coat layer containing peripheral blood mononuclear cells (PBMCs) was collected into new 50 mL conical tubes (Fisher scientific, Cat. 1443222) and centrifuged at 300 x g for 8 min, after which the supernatant was aspirated and the cell pellet consisting of PBMCs was resuspended in residual volume. Cells were washed twice by topping up the volume to 50 mL with DPBS and centrifuged at 300 x g for 8 min. The final cell pellet was resuspended in 1 mL of CryoStor® CS10 (STEMCELL™ Technologies, Cat. 07959) and kept at -80°C in Mr. Frosty Freezing Container for 24 hours, then transferred into liquid nitrogen for long-term storage.

3.2.2 Immunomagnetic enrichment of $CD14^+$ monocytes from PBMCs

On the day of the experiment, frozen PBMCs were thawed in a 37 °C water bath, then diluted at a 1:1 ratio in PLASMA-LYTE A (Baxter, Cat. JB2544) supplemented with 10% heat-inactivated cord plasma. The cell suspension was centrifuged at 300 x g for 5 min to remove the cytotoxic DMSO in the CryoStor® freezing solution. Cells were then resuspended at a concentration of 100 million cells/mL in DPBS supplemented with 2% HSA and 1mM EDTA (ThermoFisher, Cat. 15575020), followed by a positive selection of monocytes with the EasySep™ Human CD14 Positive Selection Kit II (STEMCELL™ Technologies, Cat. 17858), which conducted an immunomagnetic sorting by labeling $CD14^+$ cells with a cocktail of tetrameric antibodies targeting CD14 antigen and dextran-coated magnetic particles. Enriched $CD14^+$ monocytes were resuspended in ImmunoCult™-ACF Dendritic Cell Medium (STEMCELL™ Technologies, Cat. 10986) with the differentiation factors GM-CSF (at 50 ng/mL, PeproTech, Cat. 300-03) and IL-4

(at 35 ng/mL, PeproTech, Cat. 200-04) at a cell concentration of 1 million cells/mL to prepare the stock seed culture.

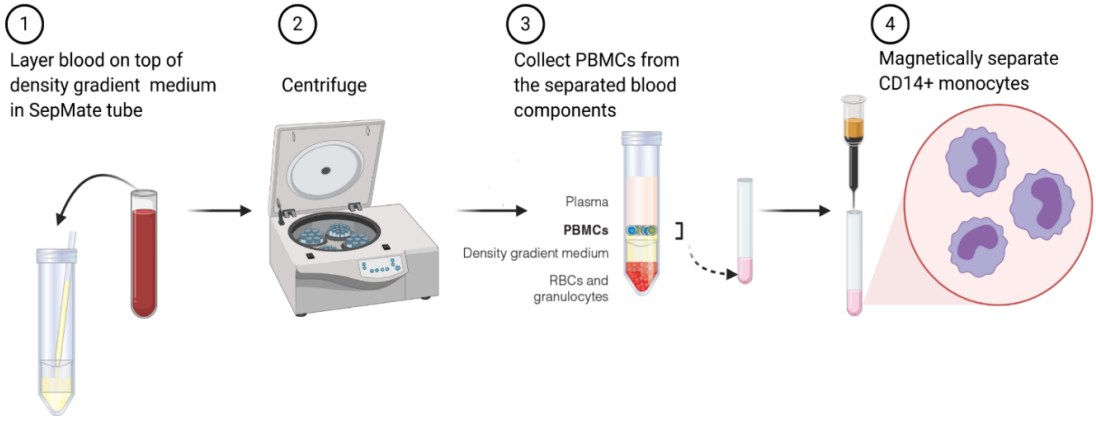

Figure 3-2 Monocyte enrichment from peripheral whole blood by Ficoll density gradient centrifugation followed by CD14$^+$ immunomagnetic sorting. Created with BioRender

3.2.3 Assessment of monocyte enrichment efficiency

Following each monocyte isolation, a small volume of the cell suspension (containing approximately 100,000 cells) was collected for assessing the frequency of CD14$^+$ monocytes in the enriched cell populations. Cells were first resuspended in 100 µL of DPBS and incubated with Fixable Viability Stain 660 for 10 min in the dark on ice. Cells were then washed twice by centrifuging at 300 x g for 5 min and resuspended in 100 µL of FACS buffer (0.1% sodium azide, 3% HI-FBS in DPBS). Afterwards, cells were incubated with Fc block for 10 min and then stained with FITC mouse anti-human CD14 antibody for 20 min in the dark on ice. Table 3-2 details the reagent information and usage as per the manufacturer's recommendations. Stained cells were analyzed using a BD Accuri™ C6 flow cytometer. Only enriched cell populations with a CD14$^+$ frequency > 85% were cultured for experiments.

Table 3-2 Antibodies and reagents used for assessing monocyte enrichment efficiency

Antibody/Reagent	Clone	Supplier (Cat.)	Volume
Fixable Viability Stain 660	-	BD Biosciences (564405)	1 µL/million cells
Human Fc Block	-	BD Biosciences (564220)	5 µL/million cells
FITC-conjugated mouse anti-human CD14	MϕP9	BD Biosciences (347493)	20 µL/test

3.3 Monocyte initial adhesion on GPPC-treated FEP surfaces

3.3.1 Preparation of FEP(-), FEP(+) and GPPC-treated FEP films for cell culture

One day before the experiment, FEP(-) and FEP(+) films (Saint-Gobain) were cut into strips of approximately 5.5cm x 2.5cm. The O-GPPC and N-hyb-GPPC-treated FEP films were removed from the -40 °C freezer inside the PECVD glove box. Each film strip was placed in a clean glass Petri dish, sealed in an autoclave pouch, and then sterilized by autoclaving (steam at 121 °C and 15 psig for 15 min). The pouches were left to cool overnight. On the day of the experiment, each film strip was carefully mounted onto the bottom of a CultureWell™ 8-well removable chamber slide (Gracebio, Cat.103541) or an 18-well sticky-slide (Ibidi, Cat. 81818) under sterile conditions.

Table 3-3 Culture plates and chamber slides used in experiments and their corresponding seeding volumes to maintain a constant seeding density of 1,565 cells/mm^2 across all surfaces

Cultureware	Supplier (Cat.)	Growth area	Volume	Cells seeded
48-well TCPS(+)	Sarstedt (83.3923)	0.64 cm^2	300 µL	0.1 million
CultureWell™ 8-well removable chamber slide	Gracebio (103541)	0.98 cm^2	460 µL	0.153 million
96-well TCPS(+)	Sarstedt (83.3924.005)	0.32 cm^2	100 µL	0.05 million
18-well sticky-slide	Ibidi (81818)	0.34 cm^2	100 µL	0.05 million

3.3.2 Cell seeding

Cells were seeded at a density of 1,565 cells/mm^2 in triplicate wells onto 48-well TCPS(+) plates and CultureWell™ 8-well removable chamber slides mounted with FEP(-), FEP(+), O-GPPC and N-hyb-GPPC films. Total volume in each well was topped up to the number listed in Table 3-3 with fresh ImmunoCult™-ACF Dendritic Cell Medium and thoroughly mixed by gently pipetting up and down. Cells were incubated at 37 °C with 5% CO_2 and allowed to adhere for 2 hours and 1 day, respectively.

3.3.3 Cell enumeration of adherent vs. non-adherent populations

Following incubation, non-adherent cells from each well were aspirated and transferred into a microcentrifuge tube. The remaining unbound cells were rinsed off the surface by pipetting up and down three times with DPBS. The microcentrifuge tubes were centrifuged at 300 x g for 5 min, and cells were resuspended in minimal residue volume and counted by Trypan blue (Sigma Aldrich, Cat. T8154) staining with a Bio-Rad TC20™ Automated Cell Counter. Nuclei of adherent cells

were stained and enumerated following the live-dead staining protocol as instructed in section 3.7.1.

3.4 Adhesion strength measurement in microfluidic flow chamber

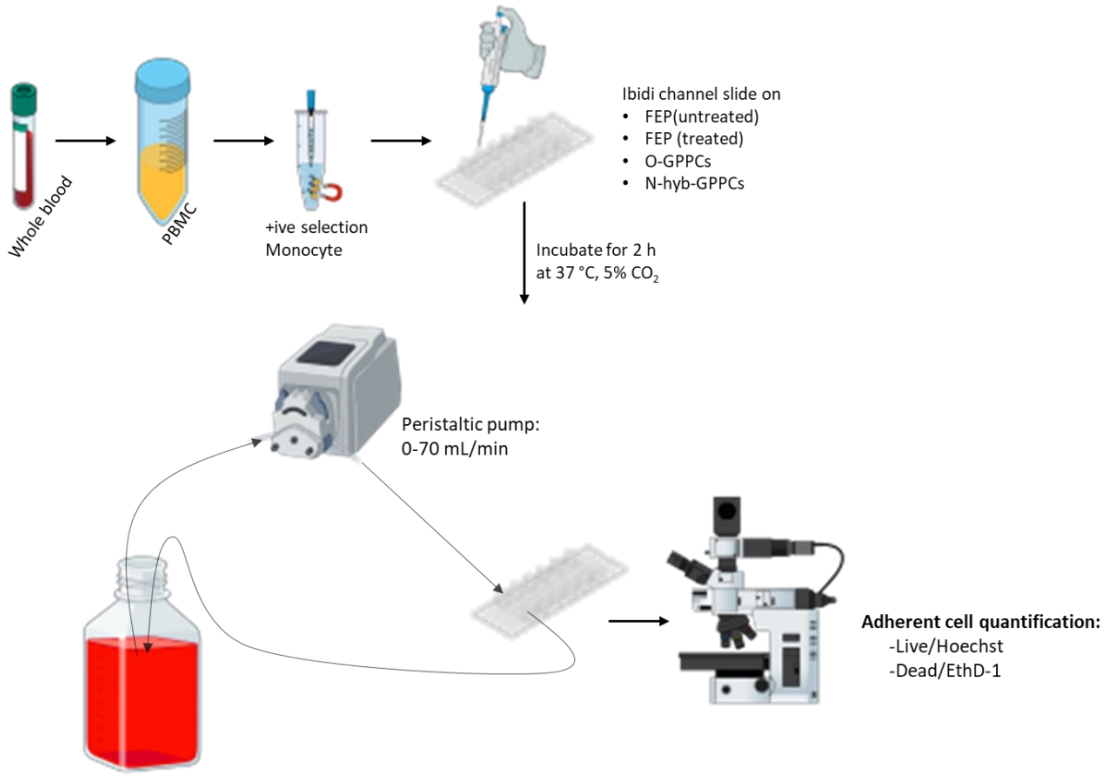

Figure 3-3 Experimental setup for testing monocyte adhesion strength under shear flow

A laminar flow with well-defined wall shear stress was applied in microfluidic flow chambers to measure the adhesion strength of monocytes on FEP-based substrates. Working seed culture was prepared at a concentration of 0.94 million cells/mL (to ensure the same seeding density as in other experiments) by diluting the stock seed culture with fresh ImmunoCult™-ACF Dendritic Cell Medium. As per the manufacturer's recommendations, 100 µL of seed culture was plated into sticky-Slide $VI^{0.4}$ flow chambers (Ibidi, Cat. 80608) mounted with FEP(-), FEP(+), O-GPPC and N-hyb-GPPC films. Cells were let to adhere for 2 hours at 37 °C and 5% CO_2. After incubation, non-adherent cells were removed by pipetting out the cell suspension, and adherent cells were stained following the live-dead staining protocol presented in section 3.7.1. The flow chambers were placed on an Olympus IX81 inverted fluorescence microscope with the chamber inlet connecting to a closed medium reservoir (filled with fresh, equilibrated DMEM at room temperature) through a peristaltic pump, and the outlet circulating back into the medium reservoir

via polytetrafluoroethylene tubing. Figure 3-3 illustrates the experimental setup. The peristaltic pump was programmed to increase flowrate from 0 to 70 mL/min at a step increment of 10 mL/min. Each flowrate was applied for 1 min, and images were acquired at the end of each 1 min time interval to monitor the detachment of cells from the surfaces under shear flow conditions. The shear stress (τ) can be calculated as a function of flowrate (ϕ) and dynamic viscosity (η) using Equation (1) which is supplied by the manufacturer.

$$\tau\left[\frac{dyn}{cm^2}\right] = \eta\left[\frac{dyn \times s}{cm^2}\right] \times 97.1 \times \phi\left[\frac{mL}{min}\right] \quad (1)$$

3.5 Immunophenotyping of monocyte integrin system

Table 3-4 Antibodies used for immunophenotyping of monocyte integrin system

Targeting antigen	Conjugate	Clone	Supplier (Cat.)	Volume/test
CD14	BV421	MΦP9	BD Biosciences (563744)	2.5 µL
CD29	APC/Cy7	TS2/16	Biolegend (303014)	5 µL
CD49c	BUV737	C3 II.1	BD Biosciences (749379)	5 µL
CD49e	BV650	IIA1	BD Biosciences (740586)	2.5 µL
CD18	BV786	6.7	BD Biosciences (743375)	2.5 µL
CD11b	PE-Cy5	M1/70	Biolegend (101210)	2.5 µL
CD11c (activated)	PE	3.9	Biolegend (301605)	2.5 µL
CD61/CD51	BUV395	23C6	BD Biosciences (744094)	2.5 µL
FcRn	AF488	937508	R&D systems (IC8639G)	2.5 µL

For surface profiling of the monocyte integrin system by flow cytometry, 100,000 freshly isolated monocytes were first incubated sequentially with Fixable Viability Stain 660 and Fc block for 10 min in the dark on ice, with two washes in between. Cells were then resuspended in 100 µL of FACS buffer and stained with antibodies in Table 3-4 for 20 min in the dark on ice. After staining, cells were washed twice by centrifuging at 300 x g for 5 min in 100 µL of FACS buffer, then fixed with the Human FoxP3 Buffer Set (BD Biosciences, Cat. 560098). Fixed cells were washed once by centrifuging at 500 x g for 5 min before being resuspended in 100 µL of FACS buffer and analyzed with a BD Fortessa flow cytometer. Flow cytometry data analysis was performed using FlowJo V.10.1. Gating strategies were illustrated in Figure 3-4. Of note:

- Expression levels of surface markers were measured by the Median Fluorescence Intensity (MFI). Relative expression levels were obtained by dividing MFIs of the stained sample over MFIs of the donor-matched unstained control.

- Positive/negative gates for determining population frequency expressing a receptor of interest were obtained using a Fluorescence Minus One (FMO) control.

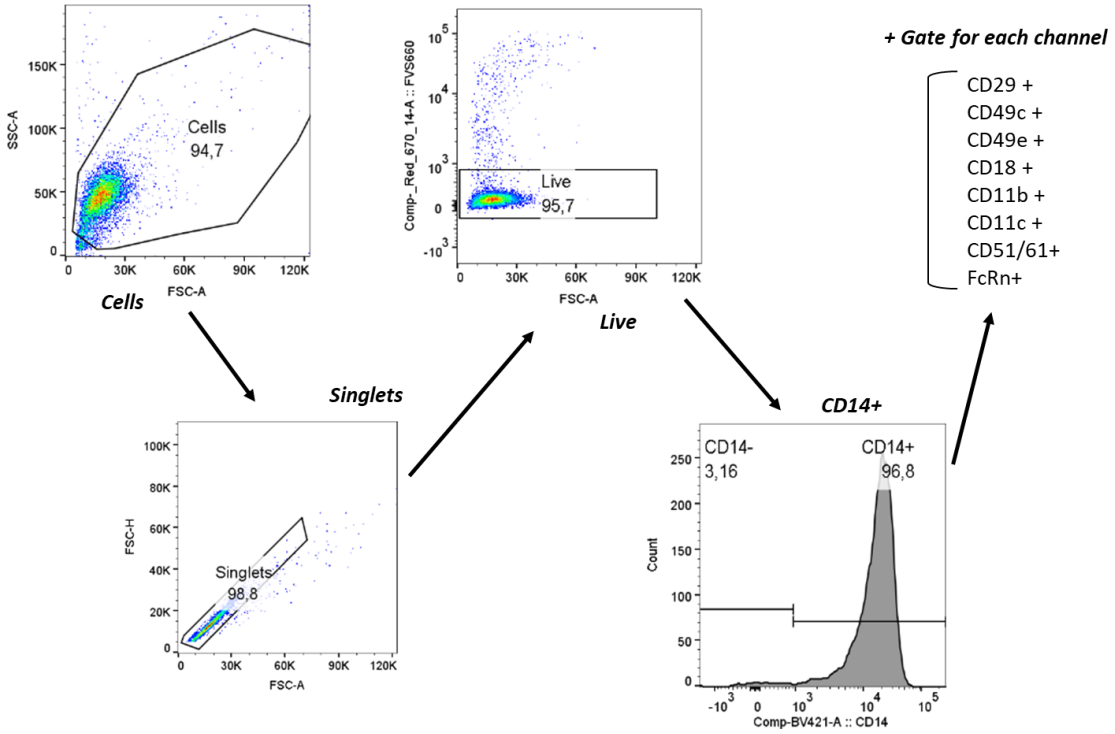

Figure 3-4 Gating strategies for immunophenotyping of monocyte integrin system

3.6 Inhibition of integrin-mediated monocyte adhesion

3.6.1 EDTA inhibition

In EDTA inhibition experiments, monocytes were seeded onto 48-well TCPS(+) plates in the presence of EDTA at concentrations of 0mM, 5mM, 10mM and 20mM. Working seed culture at each EDTA concentration was prepared by mixing appropriate volumes of stock seed culture (at 1 million cells/mL), stock EDTA solution (at 0.5M) and fresh ImmunoCult™-ACF Dendritic Cell Medium. Mixtures were incubated for 10 min at room temperature prior to cell seeding. Cells were plated onto 48-well TCPS(+) plates at 300,000 cells/well in a volume of 300 µL. Plated cells were incubated for 2 hours at 37 °C and 5% CO_2. Non-adherent cells were enumerated by Trypan blue staining as previously described in section 3.3.3. Nuclei of adherent cells were stained and imaged following the procedures in section 3.7.1.

3.6.2 RGD inhibition

The peptides CGKGGRGDS (inhibitor, referred to as RGD; BioBasic, Cat. MCGL155-3) and CGKGGRDGS (control, referred to as RDG; BioBasic, Cat. MCGL155-4) were reconstituted in DMSO at 500 mg/mL and stored at -20 °C upon receipt. In RGD inhibition experiments, monocytes were seeded onto 96-well TCPS(+) plates and 18-well sticky-slides mounted with FEP(-), FEP(+), O-GPPC and N-hyb-GPPC films in the presence of RGD or RDG peptide at concentrations of 0 mg/mL, 1 mg/mL and 5 mg/mL. Peptides were diluted to the working concentrations by mixing with stock seed culture and fresh ImmunoCult™-ACF Dendritic Cell Medium. Cells were incubated with the peptides for 30 min at room temperature prior to seeding at volumes listed in Table 3-3. Plated cells were incubated for 2 hours at 37 °C and 5% CO_2, followed by removal of the non-adherent cells from the surface by rinsing with DPBS. Adherent cells were stained and enumerated as instructed in section 3.7.1.

3.6.3 Inhibition of individual integrins using monoclonal antibodies

Cells were first incubated with Fc block at 5 µL/million cells for 10 min to block nonspecific binding, then incubated individually with blocking antibodies or isotype controls listed in Table 3-5 at a concentration of 10 µg/mL for 1 hour at room temperature. Next, cells were plated onto 96-well TCPS(+) plates and 18-well sticky-slides mounted with FEP(-), FEP(+), O-GPPC and N-hyb-GPPC films and allowed to adhere for 2 hours at 37 °C and 5% CO_2. Of note, all antibodies have been mapped to target epitopes that lie within or near the ligand binding pockets of integrins. All antibodies have also been reported as exhibiting neutralizing or adhesion blocking effects in the literature.

After incubation, non-adherent cells were aspirated out and loosely attaching cells were removed by gently rinsing the surface with DPBS. Adherent cells were incubated overnight with freshly prepared ImmunoCult™-ACF Dendritic Cell Medium containing 10% water-soluble tetrazolium 8 (WST-8, Abcam, Cat. Ab228554) at 37 °C and 5% CO_2 protected from light. Following the overnight incubation, absorbances were measured at the 460 nm wavelength with a Bio-Rad Benchmark Plus microplate spectrophotometer. The inhibitory effect of blocking antibodies was measured by normalizing the absorbance of cell sample containing the corresponding antibody to that of the negative control (i.e. cell sample without blocking antibody).

Table 3-5 Monoclonal antibodies used for inhibiting integrin-mediated monocyte adhesion

Antibody	Isotype	Clone	Supplier (Cat.)
Anti-CD29	Rat IgG2ak	mAb13	Millipore Sigma (MABT821)
Anti-CD49e	Rat IgG2ak	mAb16	Millipore Sigma (MABT820)
Anti-CD18	Mouse IgG1k	TS1/18	Biolegend (302102)
Anti-CD11b (activated)	Mouse IgG1k	CBRM1/5	Biolegend (301402)
Anti-CD11c (activated)	Mouse IgG1k	3.9	Biolegend (301602)
Mouse IgG1k Isotype	-	MOPC-21	Biolegend (400102)
Rat IgG2ak Isotype	-	RTK2758	Biolegend (400502)

3.7 Fluorescent microscopy

3.7.1 Live-dead staining for cell enumeration and cell viability

Adherent cells were incubated for 15 min in the dark with a staining mixture of Hoechst 33342 (ThermoFisher, Cat. H3570) and Ethidium homodimer-I (Abcam, Cat. ab145323) both diluted 1:400 in DPBS. Hoechst 33342 stains the nuclei of all adherent cells whereas Ethidium homodimer-I stains only nuclei of dead cells with compromised cell membranes. Stained cells were gently washed by rinsing once with DPBS, then conserved in fresh medium and imaged immediately while the cells were alive. The viability of adherent cells was tabulated by using Equation (2).

$$\%\ viable\ adherent\ cells = \frac{Hoechst\ nuclei\ counts - Ethidium\ nuclei\ counts}{Hoechst\ nuclei\ counts} \qquad (2)$$

3.7.2 Immunofluorescence staining of adhesome proteins

Adherent cells were fixed and permeabilized simultaneously for 15 min in 4% paraformaldehyde (powder dissolved in DPBS, Fisher scientific, Cat. O4042-500) containing 0.1% Triton™ X-100 (Sigma, Cat. T8787). After three washes with DPBS, cells were incubated with Dako protein block (Agilent Technologies, Cat. X090930-2) for 30 min at room temperature. Next, cells were stained with primary antibodies diluted in Dako antibody diluent (Agilent Technologies, Cat. S302283) at 4 °C overnight. On the next day, cells were washed twice with 0.05% Tween-20 (Sigma, Cat. P9416) washing buffer, followed by secondary antibody staining for 2 hours at room temperature. Table 3-6 details the primary and secondary antibody information and corresponding dilutions. Subsequently, cells were stained with 1 mg/mL 4',6-diamidino-2-phenylindole (DAPI, Sigma, Cat. D9542) diluted in RO water, then washed twice with Tween-20 washing buffer. All liquid content was aspirated from the plates and the FEP film was carefully disassembled from the removable

chamber slide. Finally, the film was mounted onto a coverslip with 50 µL of Vectashield® (Vector laboratories, H-1000) and preserved at 4 °C in the dark until imaging.

Table 3-6 Antibodies used for immunofluorescence staining of surface-adhered monocytes

	Panel 1		Panel 2	
Primary Antibodies	Mouse anti-human vinculin *1:400 Dilution* (Sigma, V9131)	Rabbit anti-human FAK Phospho Y-397 *1:400 Dilution* (MyBiosource, MBS9431044)	Rabbit anti-human FAK Phospho Y-397 *1:400 Dilution* (MyBiosource, MBS9431044)	AF555 Plus-Phalloidin *1:400 Dilution* (LifeTechnologies, A30106)
Secondary Antibodies	Goat anti-mouse AF488 *1:200 Dilution* (ThermoFisher, A11017)	Goat anti-rabbit AF546 *1:200 Dilution* (ThermoFisher, A11010)	Goat anti-rabbit AF488 *1:200 Dilution* (ThermoFisher, A11008)	

3.7.3 Image acquisition

Fluorescent image acquisition was performed with MetaMorph® version 7.10.4 on an Olympus IX81 microscope equipped with three filter sets: [Excitation filter (Ex): 398/11, Dichroic mirror (DM): 409, Emission filter (Em): 457/25], [Ex: 482/35, DM: 506, Em: 536/40] and [Ex: 525/40, DM: 555, Em: 585/40]. The center of the well was located by eye and assigned as the origin of the imaging coordinates. For enumeration of the nuclei of adherent cells, images were acquired using the 10X objective at 21 positions starting from the origin at evenly spaced intervals for 48-well TCPS(+) plates and 8-well chamber slides, or at 12 positions for 96-well TCPS(+) plates and 18-well sticky-slides. For imaging the immunofluorescence-stained adhesome structures, images were taken through the 60X objective (oil immersion) at 5 nonoverlapping positions per well.

3.7.4 Image analysis

ImageJ version 1.8.0 (National Institutes of Health and the Laboratory for Optical and Computational Instrumentation) was used for all image analysis. All macros used for automating image processing were written by the author of this thesis. To be noted, methods for quantifying FAs were adapted from Horzum *et al*[73].

3.8 Statistical analysis

Statistical analyses were performed using Graphpad© Prism software, except for the two one-sided t-tests (TOST) equivalence test and power analysis presented in Section 4.1.1 and Figure S-0-1, which were conducted with JMP Pro 16.1.0. Unless otherwise mentioned, data is reported as average ± standard error of the mean (SEM) of 3 experimental replicates from independent donors. Statistical significances were assessed with analysis of variance (ANOVA) followed by a Tukey post hoc test. Significance denotations are: ns (non-significant), * (p-value <0.05), ** (p-value <0.01), *** (p-value <0.001), **** (p-value <0.0001).

3.9 Graphical illustrations

Unless otherwise mentioned, graphical illustrations were made with Biorender online software (https://biorender.com/).

4 RESULTS AND DISCUSSIONS

4.1 Effect of surface treatment on monocyte initial adhesion to FEP substrates

4.1.1 No significant difference was observed in monocyte initial adhesion on GPPCs & FEP(+) compared to TCPS(+)

To study the effect of surface treatment on the adhesion behavior of facultative adherent cells at the substrate interface, monocytes were cultured on FEP(-), FEP(+), TCPS(+), O-GPPC and N-hyb-GPPC-treated FEP films for 2 hours (initial adhesion phase) and 1 day (early differentiation phase). Monocytes initially adhered to all surfaces at the 2-hour mark with no significant qualitative differences in cell morphology (Figure 4-1A). Immunofluorescence staining of the adhesome proteins indicated that monocytes initially adhered to all four FEP-based substrates through the formation of focal adhesions, revealing the involvement of integrins in the initial adhesion of monocytes to FEP (Figure 4-1B).

Quantification of total (Hoechst) and viable (exclusion of Ethidium homodimer-I) cells via nuclei staining showed trends consistent with observations in the phase contrast images. At 2 hours, both Saint-Gobain's proprietary surface treatment (i.e. FEP(+)) and our in-house-developed GPPCs enhanced monocyte initial adhesion in comparison to FEP(-). The highest viable adherent cell count was seen on FEP(+), followed by O-GPPC, and finally TCPS(+) and N-hyb-GPPC (Figure 4-2A). To determine whether the GPPCs and FEP(+) were practically equivalent to TCPS(+), a TOST equivalence test was conducted. TCPS(+) and the treated FEP surfaces reached practical equivalency when considering 20% differences as cutoff (Figure S-0-1 in Appendix). Based on the differences observed, cell adhesion on FEP(+) and O-GPPC can be considered as practically equivalent to the adhesion observed on TCPS(+). Cell adhesion on N-hyb-GPPC was slightly lower than on TCPS(+). However, the difference was not statistically significant, and would require at least 689 experimental replicates to detect a difference (with 95% confidence according to a power analysis), implying that it's not realistically possible to detect a practical difference between N-hyb-GPPC and TCPS(+). Similar to the viable adherent cell enumeration, no significant difference was observed in total cell yield (viable adherent cells plus viable suspension cells) on FEP(+), O-GPPC and N-hyb-GPPC compared to TCPS(+) (Figure 4-2A). While not statistically significant, cell viability on FEP(-) was lower (83.3±4.3%) compared to the other treated surfaces (>90%).

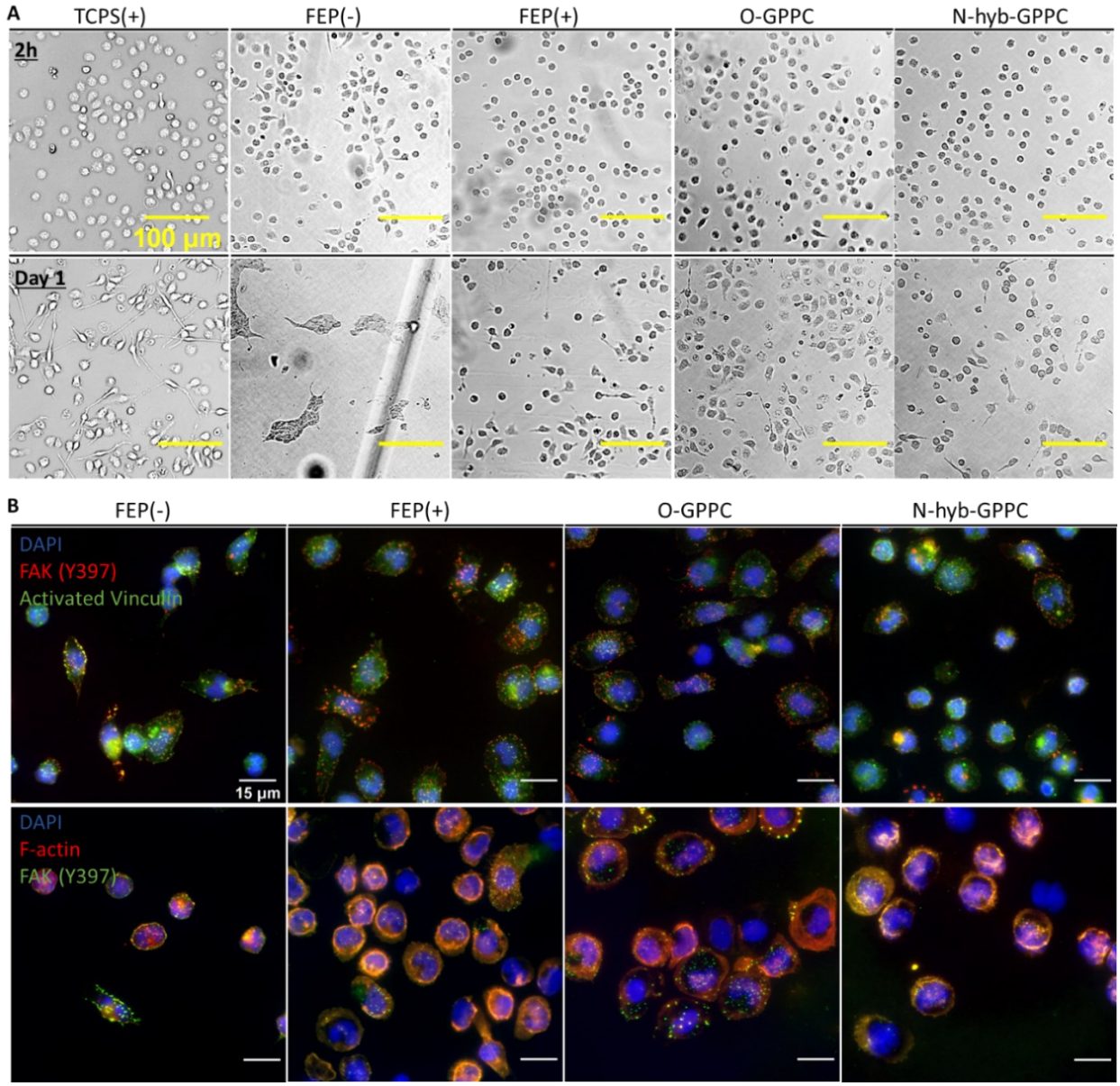

Figure 4-1 Morphology of surface-adhered monocytes. ***(A)*** *phase contrast images of monocytes adhering on TCPS(+), FEP(-), FEP(+), O-GPPC and N-hyb-GPPC at 2 hours and day 1, respectively. Scale bar represents 100 µm.* ***(B)*** *immunofluorescence images of monocytes adhering on FEP(-), FEP(+), O-GPPC and N-hyb-GPPC at 2 hours. Top row: cells were stained with DAPI (nuclei, blue), F-actin (red), and FAK at Y397 (green). Bottom row: cells were stained with DAPI (nuclei, blue), FAK at Y397 (red), and activated vinculin (green). Scale bar represents 15 µm.*

To study the effect of surface treatment on monocyte cytoskeletal organization during initial adhesion, cell spreading was measured by phalloidin labeling of filamentous actin (F-actin). FEP(+), N-hyb-GPPC and O-GPPC all significantly enhanced cell spreading in comparison to FEP(-), with the highest cell spreading being observed on O-GPPC at an average area of 316±8 μm^2 per single cell, a ~2.5-fold increase over FEP(-). Monocytes adhering to O-GPPC also formed a significantly higher number of focal adhesions (assessed by quantifying phosphorylated focal adhesion kinase (FAK) at Y397), potentially suggesting a greater extent of involvement of integrins on O-GPPC. Together, these results demonstrated the enhanced cell-surface interaction on FEP(+), N-hyb-GPPC and O-GPPC in terms of increased cell adhesion, cell spreading and adhesome formation, making them competitive with TCPS(+). In particular, O-GPPC seemed to outperform FEP(+) and N-hyb-GPPC.

Although monocyte initial adhesion was lowest on FEP(-), it is worth noting that a significant fraction comprising 33±6% of the seeded cells adhered, consistent with observations elsewhere[5,6]. Instead of facilitating adsorption of adhesive proteins, hydrophobic FEP(-) favors globular proteins such as albumin which is a major component of most serum-free cell culture media. In addition, monocytes express albumin-binding neonatal Fc (FcRn) receptors, which might be an explanation for the observed adhesion of monocytes on FEP(-)[74,75]. In situations of reduced availability of adhesive proteins on hydrophobic substrates, monocyte adhesion may proceed alternatively through FcRn receptor binding to albumin adsorbing favorably on hydrophobic surfaces.

After 1 day, monocytes adhering on FEP(-) formed clusters that were firmly attached to the surface. Conversely, cells that adhered to the other four surfaces were spread out evenly over the surface and started to form pseudopods or other membrane protrusions more characteristic of dendritic cells (Figure 4-1A). Interestingly, a decreased monocyte adhesion over time from 2 hours to day 1 was noticed, indicating a progressive detachment of monocytes from the substrates as differentiation proceeded. This observation was consistent with previous studies reported elsewhere[5,52,58].

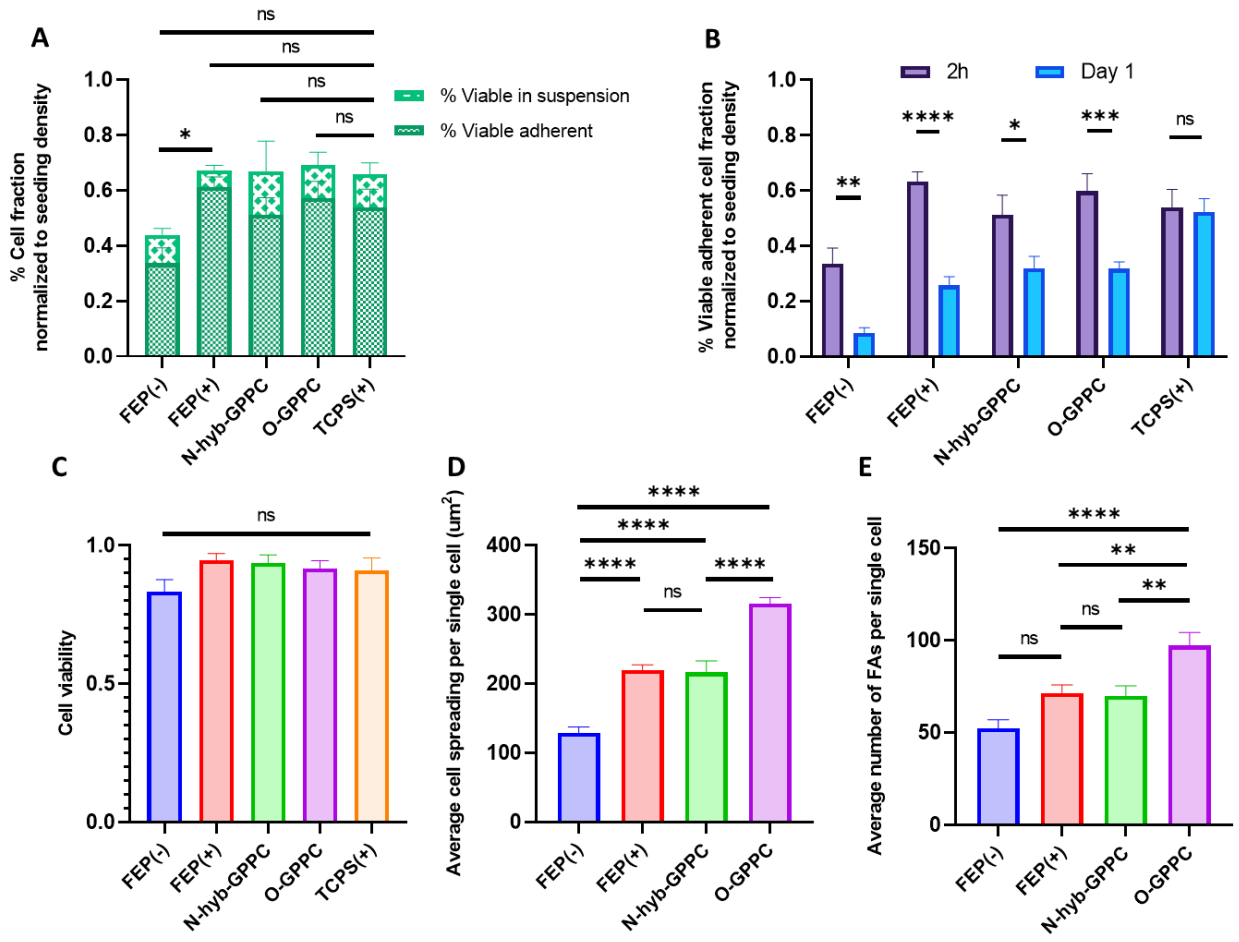

Figure 4-2 Monocyte initial adhesion on TCPS(+), FEP(-), FEP(+), O-GPPC and N-hyb-GPPC. ***(A)*** *viable cell yield on each surface after 2 hours.* ***(B)*** *cell adhesion at 2 hours vs. day 1.* ***(C)*** *viability of adherent cells on each surface after 2 hours.* ***(D)*** *average cell spreading on FEP(-), FEP(+), O-GPPC and N-hyb-GPPC after 2 hours.* ***(E)*** *average focal adhesion formation on FEP(-), FEP(+), O-GPPC and N-hyb-GPPC after 2 hours. (A-C): N=3 biological replicates with technical duplicates. (D-E): N=35 cells from 2 different biological replicates.*

4.1.2 GPPC treatment enhanced monocyte initial adhesion strength to FEP

Pipetting during media exchange and cell harvesting steps of the Mo-DC culture in FEP bags creates fluid flow. To probe the adhesion strength of cells in conditions mimicking these steps, a laminar flow with increasing shear stress at uniform step increments was applied to cells cultured in micro-scale flow chambers. Cell detachment as a function of wall shear stress was monitored by time-lapse imaging of the adherent cell nuclei.

Cells adhering on FEP(-) began to detach from the surface spontaneously as the laminar flow started. After 1-min exposure to flow at 10 mL/min (corresponding to a shear stress of 7.8 dyn/cm^2), over 60% of the initially adherent cells were removed from the surface. As the applied wall shear stress increased, this reduction in cell adhesion progressed until it gradually plateaued and reached a final cell retention rate of 15±6% at the highest tested wall shear stress. On the other hand, cell detachment on N-hyb-GPPC, O-GPPC and FEP(+) was significantly lower in comparison to FEP(-). Similar to FEP(-), the most adherent cell reduction occurred during the first flow step increment but at a minimal amount when contrasted with the FEP(-). Cells flushed away during this period were likely to be loosely attaching cells instead of firmly adherent cells with well-established adhesome structures. The vast majority of adherent cells were retained as the wall shear stress continued increasing stepwise. The final cell retention rate on N-hyb-GPPC, O-GPPC and FEP(+) was 84±5%, 79±3% and 69±7%, respectively. Of note, cell detachment from FEP(+) was greater than from N-hyb-GPPC and O-GPPC, though the difference was not statistically significant.

As stated earlier, a significant fraction of monocytes adhered to the hydrophobic FEP(-). These cells, however, seemed to adhere with weak adhesion strength. On the contrary, monocytes on N-hyb-GPPC, O-GPPC and FEP(+) were firmly adhering and were capable of withstanding high shear stresses. These results suggested that surface treatments, particularly N-hyb-GPPC and O-GPPC, not only enhanced cell adhesion, but also promoted adhesion with elevated adhesion force.

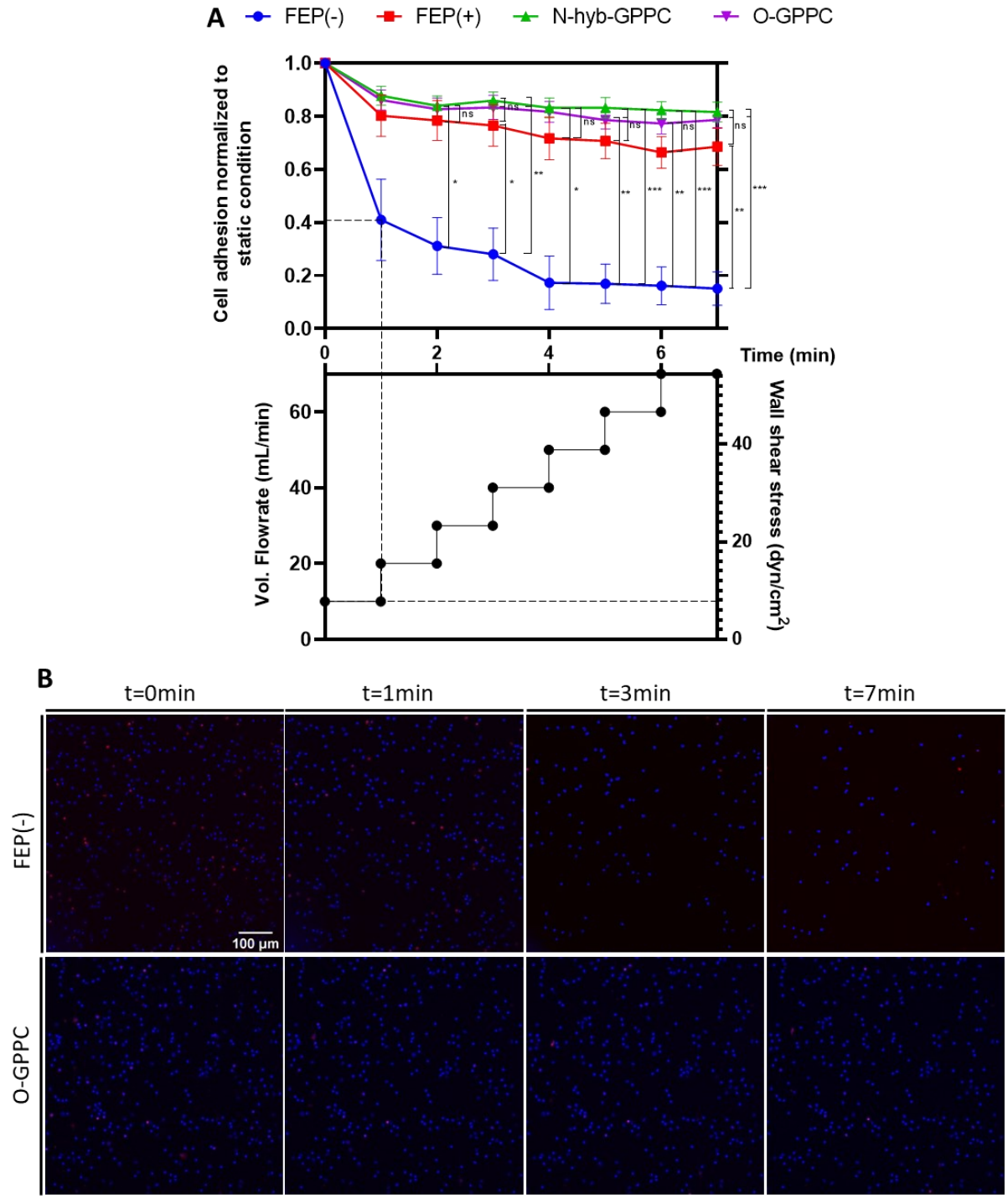

Figure 4-3 Cell adhesion on FEP(-), FEP(+), O-GPPC and N-hyb-GPPC under flow. ***(A)*** *monocyte adhesion normalized to static condition (t=0 min, 0 mL/min) as a function of time and the corresponding flowrate and wall shear stress, N=3 biological replicates with technical duplicates. Significance was assessed by a two-way repeated measures ANOVA.* ***(B)*** *Representative time-lapse images of cells at t=0 min, 1 min, 3 min and 7 min on FEP(-) and O-GPPC. Cells were stained with Hoechst 33342 (total cell nuclei, blue) and Ethidium homodimer-I (dead cell nuclei, red). Scale bar represents 100 µm.*

4.2 Effect of EDTA on monocyte initial adhesion inhibition

Based on the focal adhesion formation observed in Figure 4-1B, we hypothesized that monocyte adhesion to FEP substrates is predominately facilitated through the binding of integrins to surface-adsorbed proteins. The chelator EDTA is known to inhibit integrin-mediated adhesion by sequestering divalent cations, making them unavailable to support integrin-ligand binding. To probe our hypothesis, EDTA inhibition experiments were first conducted on TCPS(+) as a proof of concept to assess the involvement of integrins in monocyte adhesion before being extended to FEP-based substrates.

Monocytes were cultured in the presence of EDTA at different concentrations on TCPS(+) for 2 hours followed by nuclei enumeration. The addition of EDTA resulted in an obvious but non-significant adhesion reduction following a dose-dependent manner. Cell viability was assessed to ensure this observed adhesion reduction wasn't related to the cytotoxicity of EDTA (Figure 4-4A, B). Conversely, a few studies reported a complete or nearly complete inhibition of monocyte initial adhesion at 2-5 mM EDTA[52,54]. In these studies, the traditional medium formulation RPMI 1640 was used. To assess whether the choice of medium impacts the inhibitory effectiveness of EDTA, monocytes from the same donor were cultured in the presence or absence of EDTA in ImmunoCult™-ACF Dendritic Cell Medium and RPMI 1640 supplemented with 10% FBS. Culture medium was found to impact both cell initial adhesion and blocking ability of EDTA. Compared to RPMI 1640, cell adhesion was enhanced in ImmunoCult™-ACF Dendritic Cell Medium. EDTA also appeared to result in more effective inhibition in RPMI 1640 based on qualitative observations in the phase contrast images (Figure 4-4C). Since ImmunoCult™-ACF Dendritic Cell Medium is a specialized formulation specifically optimized for culturing monocytes/Mo-DCs, a possible explanation is that this medium may contain pro-adhesion peptides and/or higher quantities of divalent cations which could blunt EDTA-induced adhesion blocking.

Despite the relatively small magnitude of inhibition in our studies, a decreasing trend in monocyte initial adhesion with increasing EDTA concentration was observed. This observation indicated that integrins or other divalent cation-dependent receptors likely played a role in monocyte adhesion mechanisms. However, EDTA is a general blocking agent which does not inform the specific entities of integrins implicated in the adhesion process.

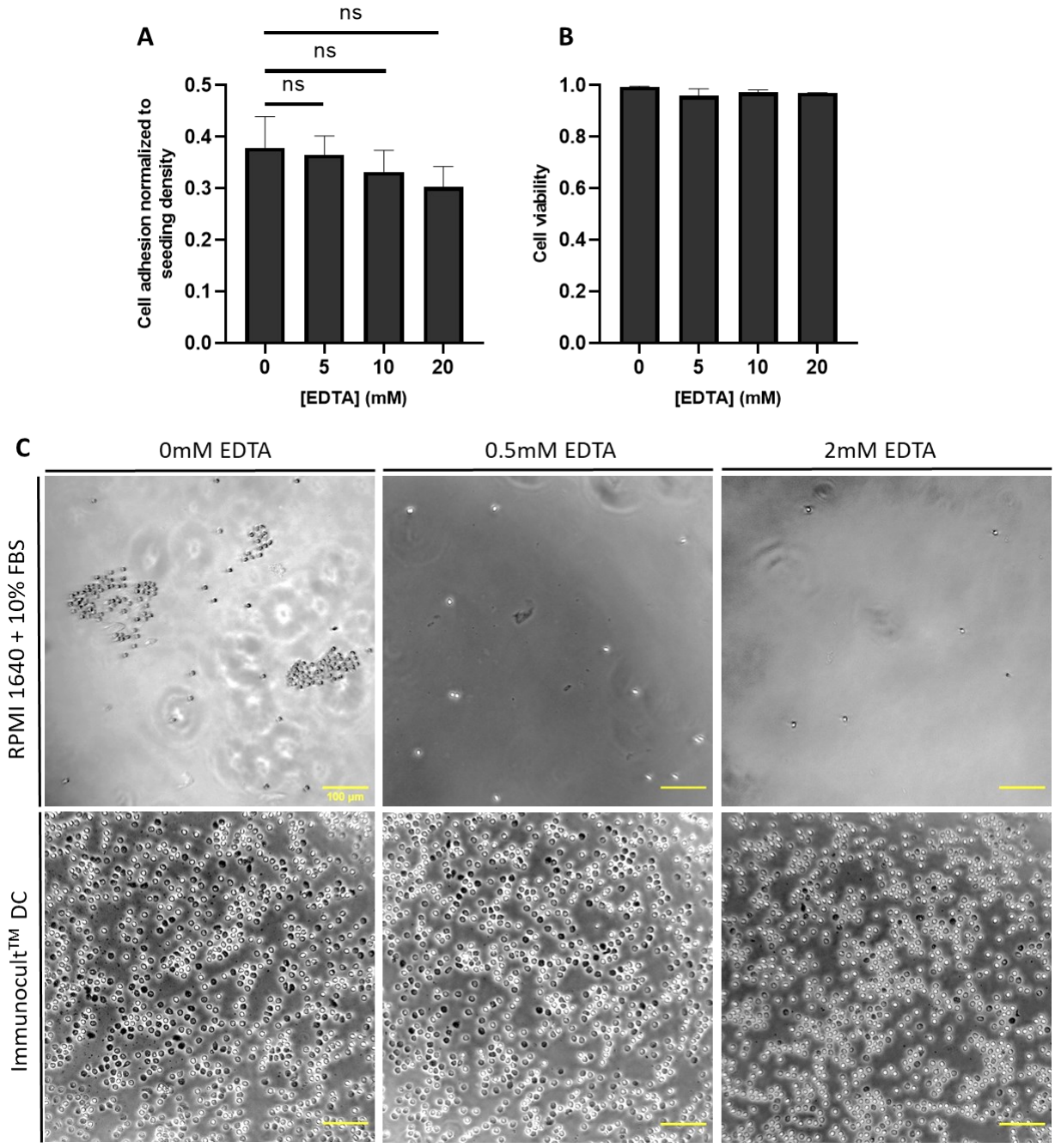

*Figure 4-4 EDTA inhibition of monocyte adhesion on TCPS(+). **(A)** cell adhesion as a function of EDTA concentration, N=3 biological replicates. **(B)** viability as a function of EDTA concentration as measured by the ratio of ethidium homodimer negative cells to total Hoechst-stained nuclei, N=2 biological replicates. **(C)** phase contrast images of adherent monocytes in RPMI 1640 + 10% FBS (top row) and ImmunoCult™-ACF Dendritic Cell Medium (bottom row) at 0, 1, 2 and 5 mM EDTA. Scale bar represents 100 µm.*

4.3 Effect of RGD-induced inhibition of monocyte initial adhesion

To determine the entities of integrins implicated in the adhesion process, inhibition experiments with more specific blocking agents were performed. The tripeptide motif RGD is another commonly used blocking agent with target specificity towards the RGD-binding integrin subfamily. RGD motifs are ubiquitously expressed in ECM proteins such as fibronectin, fibrinogen and vitronectin, and are known as the principal integrin-binding domain in these proteins[76]. In fact, 3 out of the 8 integrins expressed by monocytes (CD29/CD49c, CD29/CD49e, and CD61/CD51) were reported to recognize the RGD motif. Unlike EDTA-induced blocking which proceeds through an indirect mechanism by sequestering divalent cations from the culture medium, soluble RGD peptides pre-incubated with cells directly bind to MIDAS on integrins, making those binding sites occupied and inaccessible to surface-adsorbed proteins and hence unable to mediate cell-surface adhesion after seeding.

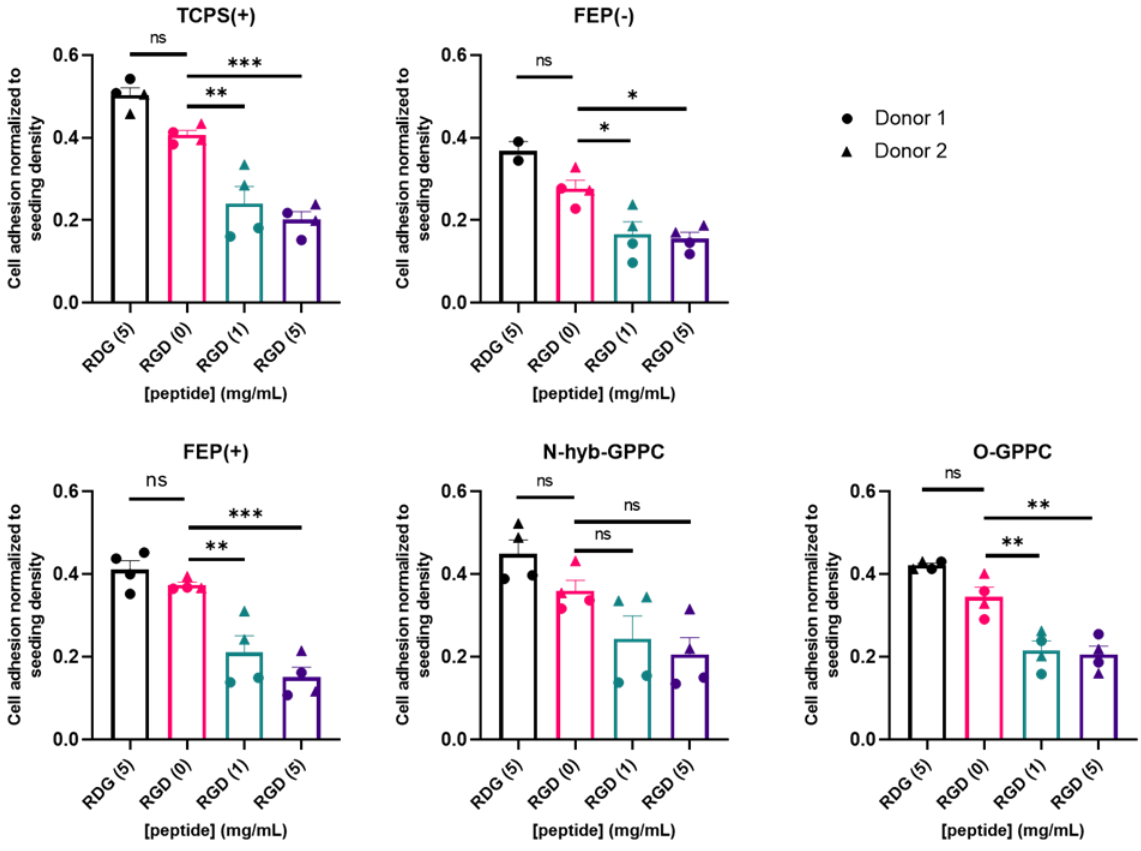

Figure 4-5 Cell adhesion on TCPS(+), FEP(-), FEP(+), O-GPPC and N-hyb-GPPC at 0, 1, 5 mg/mL of RGD and 5 mg/mL of RDG control. N=2 biological replicates with technical duplicates.

To assess whether RGD-binding integrins contribute to the adhesion mechanisms, monocytes were cultured on TCPS(+), FEP(-), FEP(+),O-GPPC and N-hyb-GPPC-treated FEP films for 2 hours in the presence of RGD at different concentrations. A control condition containing 5 mg/mL of a peptide with the same sequence except the active RGD motif being replaced by RDG was also included. The addition of RGD successfully disrupted monocyte adhesion following a dose-dependent manner on all surfaces, as shown in Figure 4-5. On the contrary, no inhibitory effect was seen in the RDG control conditions, confirming that the observed RGD-induced adhesion reduction was due to the blocking of integrins by RGD instead of the presence of a peptide in general. These results suggested that one or more of the RGD-binding integrins are implicated in the adhesion mechanisms of monocytes onto both treated and untreated FEP substrates.

4.4 Effect of selective integrin inhibition by monoclonal antibodies

Having established a potential role of the RGD-binding integrin subfamily, we next sought to identify the specific receptors within this subset which contribute to monocyte adhesion. Current information on the surface expression of monocyte integrins was compiled from studies conducted by different authors and showed discrepancies in the understanding of the surface abundance of certain integrins. Few studies have been conducted to analyze the monocyte integrin system on a global scale. Accordingly, in the context of this work, immunophenotyping of the monocyte integrin system was first conducted to confirm their surface expression. This information was then used to identify integrin receptors that might serve as cell adhesion mediators, which were subsequently blocked by monoclonal antibodies to assess their roles.

4.4.1 Monocyte surface expressions of CD18, CD11b, CD11c, CD29 and CD49e were high

Monocyte integrin receptors were selectively chosen for immunophenotyping based on their binding ligands and surface abundance reported in the literature, as presented earlier in Table 2-4. Receptors with a low likelihood of being implicated in cell-surface adhesion mechanisms due to either lack of binding to RGD motif and/or ECM proteins (i.e. CD18/CD11a, which only binds to ICAMs and contributes to cell-cell adhesion) or extremely low surface abundance reported repeatedly by different authors (i.e. CD29/CD49a and CD29/CD49d) were excluded from the analysis. Of the 8 integrins that monocytes were reported to express in literature, CD29/CD49c, CD29/CD49e, CD18/CD11b, CD18/CD11c, and CD61/CD51 were incorporated in this immunophenotyping study. Among them, CD29/CD49c, CD29/CD49e and CD61/CD51 belong

to the RGD-binding subfamily, and the remaining two belong to the leukocyte-specific β2 subfamily (the predominant integrin subfamily expressed by leukocytes including monocytes). Of note, due to the lack of well-characterized detection antibodies directed against functional integrin heterodimers, the immunophenotyping was conducted by targeting α- and β-subunit monomers separately except for CD61/CD51.

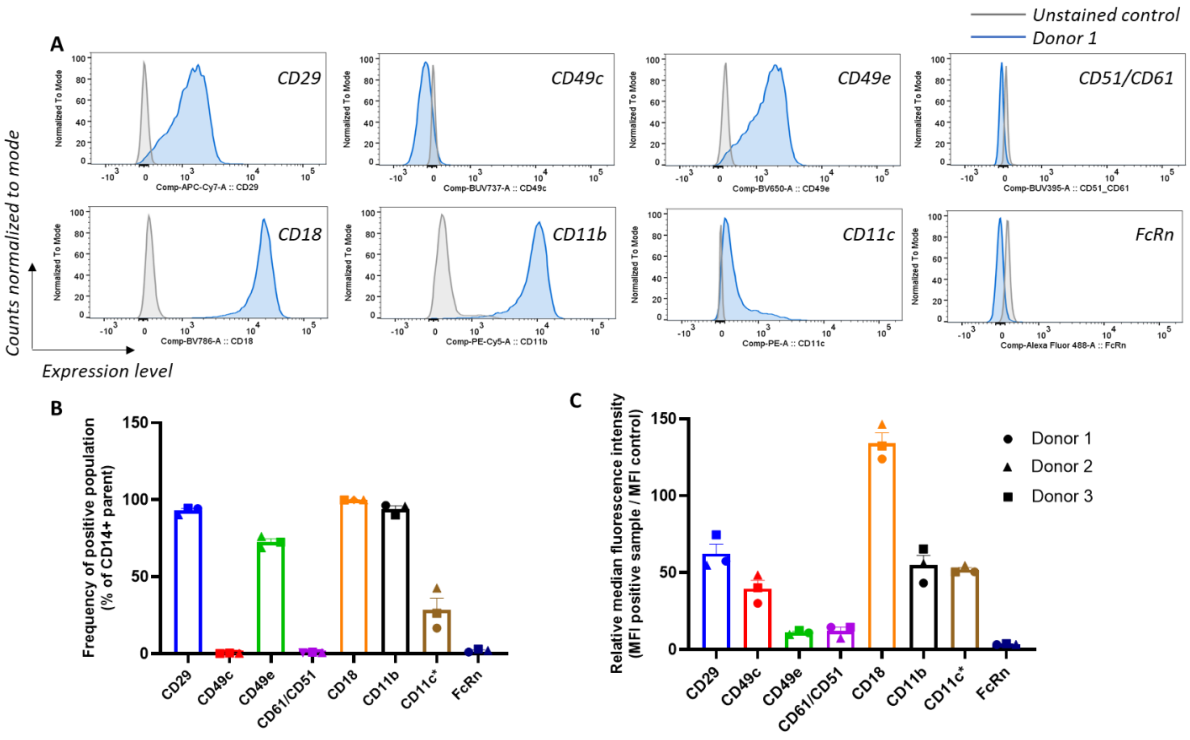

Figure 4-6 Immunophenotyping of monocyte integrin system. ***(A)*** *expression profiles of Donor 1 compared to donor-matched unstained control.* ***(B)*** *frequency of positive population.* ***(C)*** *expression level indicated by relative median fluorescence intensity (RMFI). CD11c*: detects only the activated conformation of CD11c. N=3 biological replicates.*

As illustrated in Figure 4-6B, high positive population frequencies were detected for CD29, CD49e, CD18 and CD11b. A subpopulation expressed the activated form of CD11c, which is the conformation primed for ligand-binding. Considering that activated conformation consists of only a small fraction of total integrins under equilibrium[77], the frequency of monocytes expressing CD11c regardless of conformational state was assumed to be high as well. To be noted, no significant expressions of CD49c and CD61/CD51 were detected, implying that CD29/CD49e was the only RGD-binding integrin expressed on monocyte surface, at least in our cell samples.

4.4.2 Blocking of CD29/CD49e disrupted monocyte initial adhesion to FEP substrates

Given the high surface expressions of CD29, CD49e, CD18, CD11b and CD11c which associate into three functional heterodimers CD29/CD49e, CD18/CD11b, CD18/CD11c, we hypothesized that selective blocking of these integrins would interfere with monocyte initial adhesion. Monocytes were seeded with inhibitory monoclonal antibodies targeting the α or β chain of the three aforementioned integrins at 10 μg/mL. Controls were realized by seeding monocytes 1) in the absence of any monoclonal antibody; 2) in the presence of a species and isotype-matched control. Blocking CD49e significantly disrupted monocyte initial adhesion to FEP(-), FEP(+), N-hyb-GPPC and O-GPPC by 52.2±12.5%, 37.6±11.3%, 43.6±7.3% and 61.1±4.7%, respectively. Blocking CD49e on TCPS(+) also resulted in an observable adhesion reduction by 42.8±9.2%, but the decrease was not statistically significant compared to the isotype control. Blocking the β subunit (CD29) of the CD29/CD49e heterodimer also resulted in a visible adhesion reduction on all surfaces, although the inhibitory effect was less pronounced when contrasted with blocking the α subunit (CD49e).

On the other hand, monoclonal antibodies raised against CD18 had no inhibitory effect, nor had antibodies against the α subunit CD11b or CD11c. Although CD18/CD11b and CD18/CD11c are the two most expressed integrins by monocytes, our results revealed that monocyte initial adhesion proceeded through mechanisms independent of these CD18 integrins. Conversely, the RGD-binding integrin CD29/CD49e seemed to play a significant role in facilitating cell-surface interactions. In addition, blocking of this receptor appeared to be most effective on O-GPPC, followed by N-hyb-GPPC, FEP(+) and FEP(-), and least on TCPS(+). This observation suggested that the extent to which monocyte adhesion proceeded through the CD29/CD49e-mediated mechanism was potentially higher on O-GPPC compared with the other surfaces, implying a favored adsorption of RGD motif-containing proteins to the O-GPPC substrate interface.

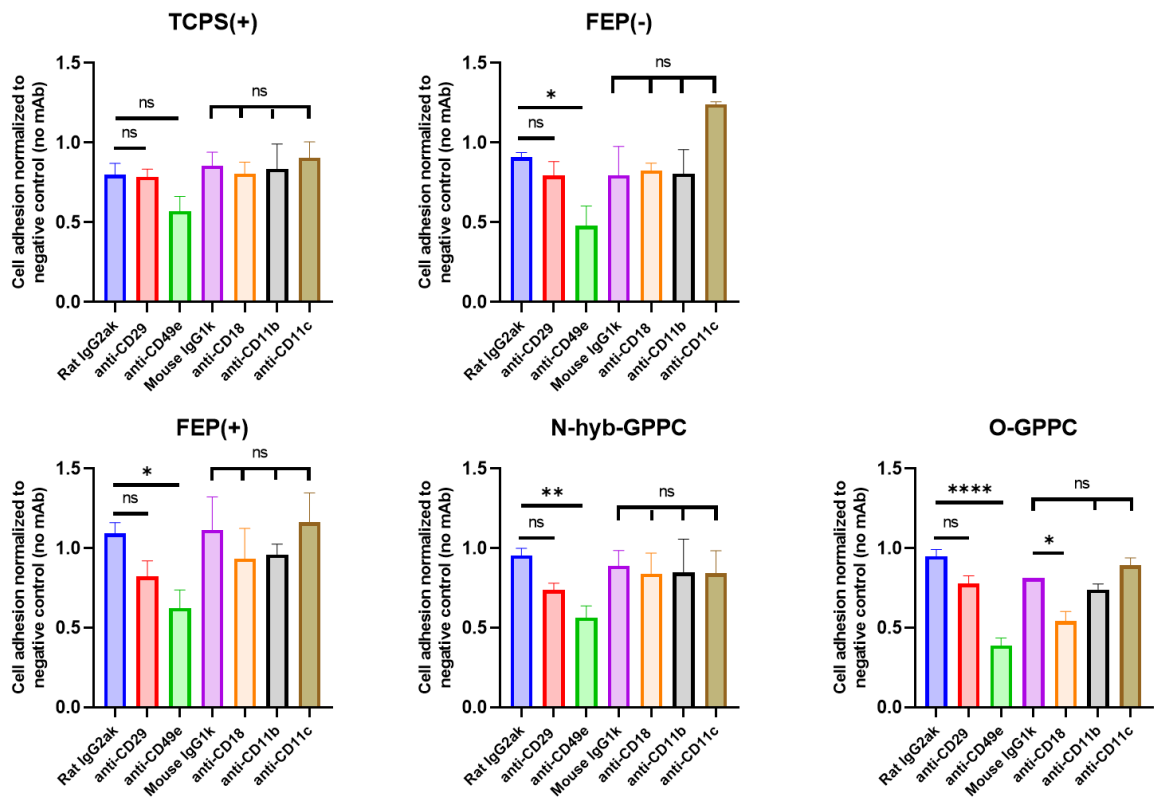

Figure 4-7 Cell adhesion on TCPS(+), FEP(-), FEP(+), O-GPPC and N-hyb-GPPC at 10 µg/mL of each blocking monoclonal antibody. N=2 biological replicates with technical duplicates.

4.5 General discussions of research findings & limitations

Altogether, the initial adhesion studies and inhibition experiments indicated that surface chemistry and culture medium together impose a combinatory effect on monocyte initial adhesion.

With plasma deposition of the GPPCs, we achieved heightened adhesion of the facultative adherent monocytes onto FEP to a level that was comparable to TCPS(+). This was accomplished with the introduction of functional groups which rendered the bio-inert FEP surfaces more hydrophilic thereby more affinitive to cell-adhesive proteins present in the culture medium. In general, surface functionalization techniques increase cell adhesion by augmenting surface adsorption of cell-adhesive proteins such as ECM proteins which facilitates cell adhesion by binding to integrins. It is expected that proteins weakly adsorb onto non-ionic FEP(-) through hydrophobic interactions and/or Van der Waals forces, whereas proteins are electrostatically attracted to localized charges on GPPCs, thereby facilitating not only elevated cell adhesion but also firm adhesion with strong force[62]. Using metrics including cell adhesion, cell spreading, focal

adhesion formation and adhesion strength, we demonstrated the ability of plasma-deposited organic coatings in modulating cell behavior at a solid substrate interface, and in helping to predict cell-surface interactions as a function of surface chemistries.

Interestingly, Corning Life Sciences recently launched the MicroDEN® for the generation of Mo-DCs in a novel, closed and automated perfusion system composed of TCPS. Immature Mo-DCs generated in the MicroDEN® system were phenotypically and functionally equivalent to those produced in plates using conventional protocols, proving successfully the concept of generating Mo-DCs in perfusion cultures where manual manipulations such as medium exchanges were avoided[78]. Our GPPCs with heightened adhesion strength and cell retention under shear flow present promising avenues for developing functional FEP bag systems where leukapheresis, monocyte capture (by plastic adherence), and differentiation into Mo-DCs under perfusion could all be achieved in fully closed settings, while at the same time benefiting from the scalability of FEP bags owing to their exceptional polymeric properties.

Additionally, O-GPPC seemed to outperform N-hyb-GPPC. Carboxylic groups on O-GPPC possess a negative charge at physiological pH and preferentially bind to proteins with a positive net charge, whereas aminated N-hyb-GPPC surface is positively charged and attracts proteins with a negative net charge. Although the composition of ImmunoCult™-ACF Dendritic Cell Medium remains the trade secret of the manufacturer, we could hypothesize that the prominent cell-adhesive proteins present in the medium are likely to be positively charged which adsorb favorably on O-GPPC.

Our inhibition experiments with a series of blocking reagents including EDTA, RGD peptide and monoclonal antibodies revealed the importance of integrins in mediating monocyte initial adhesion. In particular, we identified the RGD-binding integrin CD29/CD49e as a pivotal adhesion mediator in serum-free medium. Previous studies on monocyte adhesion mechanisms to culture vessel substrates were mostly focused on the CD18-dependent pathways since integrins in this subfamily are predominantly expressed on monocytes. Many of these studies reported a significant inhibitory effect by anti-CD18 and/or anti-CD11b, anti-CD11c monoclonal antibodies[53,54,56], but a few also reported limited or minimal inhibition by blocking these two receptors similar to our results[55,57]. Interestingly, Orgovan *et al.* studied monocyte adhesion onto surfaces coated with fibrinogen or a biomimetic copolymer PLL-g-PEG-RGD[58]. In their studies, fibrinogen-coated surfaces were

found to be more efficient in promoting monocyte adhesion despite having fewer RGD sites than the biomimetic copolymer. This observation suggested that other adhesive binding sites present in fibrinogen were competing with RGD motifs, and in fact played a more decisive role in binding to integrins.

In our case, ImmunoCult™-ACF Dendritic Cell Medium is a serum-free and chemically defined formulation devoid of plasma proteins such as fibrinogen. This might explain why CD18 integrins did not implicate in monocyte initial adhesion in our studies. Considering our results and those reported by others, one hypothesis is that monocyte adhesion proceeds through alternative integrin-mediated mechanisms depending on the available proteins present in the culture medium or secreted by the cells. In the presence of plasma proteins such as fibrinogen and fibronectin which are known as the major ligands for CD18/CD11b and CD18/CD11c, monocyte initial adhesion is likely primarily dominated by the CD18 integrins due to their abundance on the monocyte cell surface, whilst our results demonstrated that monocyte adhesion proceeds through CD18-independent mechanisms with CD29/CD49e as a major cell adhesion mediator in serum-free media.

This finding has important implications for understanding the downstream signaling pathways that are triggered during the adhesion process, which will help us uncover the long-existing puzzle: Is plastic adherence beneficial for the differentiation and maturation of monocytes into Mo-DCs[2]? Of note, a few authors have demonstrated the critical roles played by integrins in deciding the cell fate of monocytes and/or monocyte-derived cell products[59,60,79,80]. For example, Gonzalez *et al.* observed that binding of CD61/CD51 and CD29/CD49e to plasma proteins drove the monocyte-to-DC conversion in extracorporeal photochemotherapy[59]. Rezzonico *et al.* reported that ligation of CD11b or CD11c rapidly stimulated high production of IL-1β[79]. Therefore, our improved understanding of the monocyte adhesion mechanisms constitutes the first step in the cascades to fully elucidate the impact of *in vitro* cell culture on Mo-DC therapeutic efficacy. In addition, understanding the adhesion mechanisms permits the tailoring of Mo-DC generation towards pro-adherent or pro-suspension cultures (depending on the intended application). In fact, Mo-DC generation is associated with high batch-to-batch variability, which represents one of the challenges currently faced in the field. This is, in part, a result of the poor control over cell-surface interactions in the traditional protocols. In this context, our GPPCs and knowledge of the adhesion

mechanisms will allow improved modulation of monocyte-substrate interactions, which could contribute to enhancing the clinical reproducibility of Mo-DC immunotherapies.

4.6 Recommendations for future work

To be noted, our interpretation of the results was largely limited by the unclear composition of the ImmunoCult™-ACF Dendritic Cell Medium. While the detailed composition is a trade secret of the manufacturer, it could have been useful to identify the major protein components through techniques such as proteomics analysis. In addition, we rationalized that the elevated cell adhesion on the GPPCs may be the result of a higher amount of cell-adhesive proteins adsorbed on the functionalized surfaces, whereas the lower cell adhesion on FEP(-) may be explained by the abundance of surface-adsorbed albumin attributed to the higher affinity of albumin to hydrophobic surfaces. We proposed this rationale based on the observations by Zelzer *et al.*[11], which showed that the ability of fibronectin to displace albumin in the protein adlayer is reduced on hydrophobic surfaces. To study this rationale, it would be important to identify as well as quantify the protein ligands that are present in the protein adlayer on GPPCs versus FEP(-). This could be examined by running mass spectroscopy or Western blot on the desorbed proteins from each surface, or by novel microscopy-based techniques such as the method described by Togashi *et al.*[81].

In addition to the enhanced adhesion of monocytes to GPPCs along with elevated adhesion strength that we've demonstrated, it would also be interesting to study how the GPPCs interact with monocytes in terms of cell adhesion dynamics. A number of techniques are available for studying the adhesion dynamics of cells onto a solid surface, including optical biosensor, quartz crystal microbalance with dissipation monitoring (QCM-D) and automated micropipette-based adhesion assay which were extensively described by Orgovan *et al.*[58].

Finally, our experiments focused on assessing the role played by integrins in monocyte initial adhesion. However, other integrin-independent mechanisms such as electrostatic interactions, and/or non-integrin receptor-mediated adhesion might also exist. These could also represent future directions to continue this project.

5 CONCLUSIONS

The results presented herein demonstrated the strong translational potential of the GPPCs in developing surface-functionalized FEP bags for tailoring the culture of facultative adherent cells such as monocytes towards adherent culture. Using metrics including cell adhesion, cytoskeletal organization, adhesome formation and adhesion strength, we demonstrated that both O-GPPC and N-hyb-GPPC treatments enhanced FEP surface interactions with monocytes during the initial adhesion phase, which represents the first stage in *in vitro* cell culture that plays an integral role in cell mechanotransduction and affects cell behavior, function and fate decisions[82]. In particular, both GPPCs had comparable performance to TCPS(+) in terms of promoting monocyte initial adhesion, presenting promising alternatives to open culture vessels consisting of TCPS(+). In addition, owing to the elevated adhesion strength and cell retention rate under flow presented by the GPPCs, the potential is there to develop functionally closed FEP bag systems where monocyte enrichment, differentiation and maturation into Mo-DCs could be conducted under perfusion to completely close the manufacturing system.

Our findings also supported our hypothesis that integrins were implicated in monocyte-surface interactions. Monocyte adhesion onto TCPS(+), treated and untreated FEP substrates were all primarily facilitated through integrin-mediated mechanisms irrespective of the base substrate material, but the extent to which integrins were implicated was dependent on the substrate surface chemistry. Specifically, the RGD-binding integrin CD29/CD49e was identified as a major cell adhesion mediator in the context of the works conducted in this thesis. Combining with the observation by other authors that the CD18-associating integrins (CD18/CD11b and/or CD18/CD11c) played a predominant role in monocyte initial adhesion in serum-containing medium, we came to the conclusion that monocyte adhesion likely proceeds through alternative mechanisms depending on the availability of proteins present in the culture medium. In serum-free, animal component-free media devoid of common plasma proteins such as fibrinogen and fibronectin, CD18-independent adhesion mechanisms with CD29/CD49e acting as a major cell adhesion mediator are favorably adopted by monocytes. Substrate surface chemistry and choice of medium thereby impose a combinatory effect on monocyte initial adhesion.

To the best of our knowledge, we are the first few groups to identify that monocyte-substrate adhesion proceeds primarily through CD29/CD49e-mediated mechanisms in serum-free media.

As serum-free media is now widely adopted in clinical manufacturing of Mo-DCs, this observation will pave the way for us to study the mechanotransduction and signaling pathways triggered during the adhesion process, which will help us understand the biological machinery underlying how cell-surface interactions impact the final cell fate decisions of Mo-DCs. On top of this, our improved understanding of monocyte adhesion mechanisms will inform the design and development of next-generation plasma polymer coatings or biomaterials in general to permit better control of cell behavior at the substrate interface.

REFERENCES

1. Sabbatier, G., Ramachandran, B. & Girard-Lauriault, P.-L. Method to produce stable and sterilizable coatings for cell culture/ therapy plastics. Disclosure under licensing discussions with Saint-Gobain Life Sciences.
2. Fekete, N., Béland, A. V., Campbell, K., Clark, S. L. & Hoesli, C. A. Bags versus flasks: a comparison of cell culture systems for the production of dendritic cell-based immunotherapies. *Transfusion* **58**, 1800–1813 (2018).
3. Wong, E. C. C. *et al.* Development of a closed-system process for clinical-scale generation of DCs: evaluation of two monocyte-enrichment methods and two culture containers. *Cytotherapy* **4**, 65–76 (2002).
4. Suen, Y. *et al.* Comparison of monocyte enrichment by immuno-magnetic depletion or adherence for the clinical-scale generation of DC. *Cytotherapy* **3**, 365–375 (2001).
5. Bastien, J.-P. *et al.* Closing the system: production of viral antigen-presenting dendritic cells eliciting specific CD8+ T cell activation in fluorinated ethylene propylene cell culture bags. *J Transl Med* **18**, 383 (2020).
6. Kurlander, R. J., Tawab, A., Fan, Y., Carter, C. S. & Read, E. J. A functional comparison of mature human dendritic cells prepared in fluorinated ethylene-propylene bags or polystyrene flasks. *Transfusion* **46**, 1494–1504 (2006).
7. Wilson, C. J., Clegg, R. E., Leavesley, D. I. & Pearcy, M. J. Mediation of biomaterial-cell interactions by adsorbed proteins: a review. *Tissue Eng* **11**, 1–18 (2005).
8. Harjunpää, H., Llort Asens, M., Guenther, C. & Fagerholm, S. C. Cell Adhesion Molecules and Their Roles and Regulation in the Immune and Tumor Microenvironment. *Front Immunol* **10**, 1078 (2019).
9. Wu, C. Focal adhesion: a focal point in current cell biology and molecular medicine. *Cell Adh Migr* **1**, 13–18 (2007).
10. Carré, A. & Lacarrière, V. How Substrate Properties Control Cell Adhesion. A Physical–Chemical Approach. *Journal of Adhesion Science and Technology* **24**, 815–830 (2010).
11. Zelzer, Darren Albutt, Morgan R. Alexander, & Noah A. Russell. The Role of Albumin and Fibronectin in the Adhesion of Fibroblasts to Plasma Polymer Surfaces. *Plasma Processes and Polymers* **9**,.
12. Arima, Y. & Iwata, H. Effects of surface functional groups on protein adsorption and subsequent cell adhesion using self-assembled monolayers. *J. Mater. Chem.* **17**, 4079–4087 (2007).
13. Rostam, H. *et al.* The impact of surface chemistry modification on macrophage polarisation. *Immunobiology* **221**, (2016).
14. Babaei, S., Fekete, N., Hoesli, C. A. & Girard-Lauriault, P.-L. Adhesion of human monocytes to oxygen- and nitrogen- containing plasma polymers: Effect of surface chemistry and protein adsorption. *Colloids Surf B Biointerfaces* **162**, 362–369 (2018).
15. Steinman, R. & Cohn, Z. IDENTIFICATION OF A NOVEL CELL TYPE IN PERIPHERAL LYMPHOID ORGANS OF MICE | Journal of Experimental Medicine | Rockefeller University Press. *The Journal of Experimental Medicine* **137**, (1973).
16. Filin, I. Y., Kitaeva, K. V., Rutland, C. S., Rizvanov, A. A. & Solovyeva, V. V. Recent Advances in Experimental Dendritic Cell Vaccines for Cancer. *Frontiers in Oncology* **11**, (2021).
17. Gardner, A., de Mingo Pulido, Á. & Ruffell, B. Dendritic Cells and Their Role in Immunotherapy. *Frontiers in Immunology* **11**, (2020).
18. Hopewell, E. L. & Cox, C. Manufacturing Dendritic Cells for Immunotherapy: Monocyte Enrichment. *Mol Ther Methods Clin Dev* **16**, 155–160 (2020).

19. Sipuleucel-T: APC 8015, APC-8015, prostate cancer vaccine--Dendreon. *Drugs R D* **7**, 197–201 (2006).
20. Anguille, S., Smits, E. L., Lion, E., van Tendeloo, V. F. & Berneman, Z. N. Clinical use of dendritic cells for cancer therapy. *The Lancet Oncology* **15**, e257–e267 (2014).
21. Mastelic-Gavillet, B., Balint, K., Boudousquie, C., Gannon, P. O. & Kandalaft, L. E. Personalized Dendritic Cell Vaccines—Recent Breakthroughs and Encouraging Clinical Results. *Frontiers in Immunology* **10**, (2019).
22. Palucka, K. & Banchereau, J. Cancer immunotherapy via dendritic cells. *Nat Rev Cancer* **12**, 265–277 (2012).
23. Cintolo, J. A., Datta, J., Mathew, S. J. & Czerniecki, B. J. Dendritic cell-based vaccines: barriers and opportunities. *Future Oncology* **8**, 1273–99 (2012).
24. Hu, Z., Ott, P. A. & Wu, C. J. Towards personalized, tumour-specific, therapeutic vaccines for cancer. *Nat Rev Immunol* **18**, 168–182 (2018).
25. Draube, A. *et al.* Dendritic cell based tumor vaccination in prostate and renal cell cancer: a systematic review and meta-analysis. *PLoS One* **6**, e18801 (2011).
26. Kantoff, P. W. *et al.* Sipuleucel-T immunotherapy for castration-resistant prostate cancer. *N Engl J Med* **363**, 411–422 (2010).
27. Yao, T. & Asayama, Y. Animal-cell culture media: History, characteristics, and current issues. *Reproductive Medicine and Biology* **16**, 99–117 (2017).
28. Keenan, J., Pearson, D. & Clynes, M. The role of recombinant proteins in the developmentof serum-free media. *Cytotechnology* **50**, 49 (2006).
29. Lerman, M. J., Lembong, J., Muramoto, S., Gillen, G. & Fisher, J. P. The Evolution of Polystyrene as a Cell Culture Material. *Tissue Engineering Part B: Reviews* **24**, 359–372 (2018).
30. Teng, H. Overview of the Development of the Fluoropolymer Industry. *Applied Sciences* **2**, 496–512 (2012).
31. Ebnesajjad, S. 5 - Introduction to Thermoplastic Fluoropolymers. in *Introduction to Fluoropolymers (Second Edition)* (ed. Ebnesajjad, S.) 43–61 (William Andrew Publishing, 2021). doi:10.1016/B978-0-12-819123-1.00005-7.
32. Wang, J. *et al.* Discrimination of the heterogeneity of bone marrow-derived dendritic cells. *Mol Med Rep* **16**, 6787–6793 (2017).
33. Pullarkat, V., Lau, R., Lee, S.-M., Bender, J. G. & Weber, J. S. Large-scale monocyte enrichment coupled with a closed culture system for the generation of human dendritic cells. *Journal of Immunological Methods* **267**, 173–183 (2002).
34. Yi, H.-J. & Lu, G.-X. Adherent and non-adherent dendritic cells are equivalently qualified in GM-CSF, IL-4 and TNF-α culture system. *Cell Immunol* **277**, 44–48 (2012).
35. Li, G.-B. & Lu, G.-X. Adherent cells in granulocyte-macrophage colony-stimulating factor-induced bone marrow-derived dendritic cell culture system are qualified dendritic cells. *Cell Immunol* **264**, 4–6 (2010).
36. Romani, N. *et al.* Generation of mature dendritic cells from human blood. An improved method with special regard to clinical applicability. *J Immunol Methods* **196**, 137–151 (1996).
37. Pickl, W. F. *et al.* Molecular and functional characteristics of dendritic cells generated from highly purified CD14+ peripheral blood monocytes. *J Immunol* **157**, 3850–3859 (1996).
38. Sorg, R. V. *et al.* Clinical-scale generation of dendritic cells in a closed system. *J Immunother* **26**, 374–383 (2003).
39. Atefeh Solouk, Brian Cousins, Hamid Mirzadeh, & Alexander Seifalian. Application of plasma surface modification techniques to improve hemocompatibility of vascular grafts: A review - PubMed. *Biotechnology and Applied Biochemistry* **58**,.

40. Jacobs, T., Morent, R., De Geyter, N., Dubruel, P. & Leys, C. Plasma Surface Modification of Biomedical Polymers: Influence on Cell-Material Interaction. *Plasma Chem Plasma Process* **32**, 1039–1073 (2012).
41. Babaei, S. & Girard-Lauriault, P.-L. Tuning the Surface Properties of Oxygen-Rich and Nitrogen-Rich Plasma Polymers: Functional Groups and Surface Charge. *Plasma Chem Plasma Process* **36**, 651–666 (2016).
42. Bogaerts, A., Neyts, E., Gijbels, R. & van der Mullen, J. Gas discharge plasmas and their applications. *Spectrochimica Acta Part B: Atomic Spectroscopy* **57**, 609–658 (2002).
43. Girard-Lauriault, P.-L., Desjardins, P., Unger, W. E. S., Lippitz, A. & Wertheimer, M. R. Chemical Characterisation of Nitrogen-Rich Plasma-Polymer Films Deposited in Dielectric Barrier Discharges at Atmospheric Pressure. *Plasma Processes and Polymers* **5**, 631–644 (2008).
44. H Conrads & M Schmidt. Plasma generation and plasma sources - IOPscience. *Plasma Sources Science and Technology* **9**,.
45. Osenga, G. Corona Discharge. https://www.thierry-corp.com/plasma-knowledgebase/corona-discharge.
46. Ghafouri, S. *et al.* Study on Physio-chemical Properties of plasma polymerization in C2H2/N2 plasma and Their Impact on COL X. *Sci Rep* **7**, 9149 (2017).
47. Vandenbossche, M. & Hegemann, D. Recent approaches to reduce aging phenomena in oxygen- and nitrogen-containing plasma polymer films: An overview. *Current Opinion in Solid State and Materials Science* **22**, 26–38 (2018).
48. Hegemann, D. *et al.* Suppression of Hydrophobic Recovery by Plasma Polymer Films with Vertical Chemical Gradients. *Langmuir* (2016).
49. Vandenbossche, M. *et al.* Functionality and chemical stability of plasma polymer films exhibiting a vertical cross-linking gradient in their subsurface. *Polymer Degradation and Stability* **156**, 259–268 (2018).
50. Wang, Y. *et al.* Effects of surface functional groups on proliferation and biofunction of Schwann cells. *J Biomater Appl* **30**, 1494–1504 (2016).
51. Fekete, N., Hoesli, C. & Coulombe, S. *Effects of fluoropolymer surface properties on monocyte cell fate - April 2016 Progress Report*.
52. Shen, M. & Horbett, T. A. The effects of surface chemistry and adsorbed proteins on monocyte/macrophage adhesion to chemically modified polystyrene surfaces. *J Biomed Mater Res* **57**, 336–345 (2001).
53. McNally, A. K. & Anderson, J. M. Beta1 and beta2 integrins mediate adhesion during macrophage fusion and multinucleated foreign body giant cell formation. *Am J Pathol* **160**, 621–630 (2002).
54. Garnotel, R. *et al.* Human Blood Monocytes Interact with Type I Collagen Through αxβ2 Integrin (CD11c-CD18, gp150-95). *The Journal of Immunology* **164**, 5928–5934 (2000).
55. Patarroyo, M., Prieto, J., Beatty, P. G., Clark, E. A. & Gahmberg, C. G. Adhesion-mediating molecules of human monocytes. *Cellular Immunology* **113**, 278–289 (1988).
56. McNally, A. K. & Anderson, J. M. Complement C3 participation in monocyte adhesion to different surfaces. *Proc Natl Acad Sci U S A* **91**, 10119–10123 (1994).
57. Sándor, N. *et al.* CD11c/CD18 Dominates Adhesion of Human Monocytes, Macrophages and Dendritic Cells over CD11b/CD18. *PLOS ONE* **11**, e0163120 (2016).
58. Orgovan, N. *et al.* Adhesion kinetics of human primary monocytes, dendritic cells, and macrophages: Dynamic cell adhesion measurements with a label-free optical biosensor and their comparison with end-point assays. *Biointerphases* **11**, 031001 (2016).
59. Gonzalez, A. L. *et al.* Integrin-driven monocyte to dendritic cell conversion in modified extracorporeal photochemotherapy. *Clin Exp Immunol* **175**, 449–457 (2014).

60. Brilha, S., Wysoczanski, R., Whittington, A. M., Friedland, J. S. & Porter, J. C. Monocyte Adhesion, Migration, and Extracellular Matrix Breakdown Are Regulated by Integrin αVβ3 in Mycobacterium tuberculosis Infection. *The Journal of Immunology* **199**, 982–991 (2017).
61. Wertheimer, M. R. *et al.* Amine-Rich Organic Thin Films for Cell Culture: Possible Electrostatic Effects in Cell–Surface Interactions. *Jpn. J. Appl. Phys.* **51**, 11PJ04 (2012).
62. Hoshiba, T., Yoshikawa, C. & Sakakibara, K. Characterization of Initial Cell Adhesion on Charged Polymer Substrates in Serum-Containing and Serum-Free Media. *Langmuir* **34**, 4043–4051 (2018).
63. Danen, E. H. J. *Integrins: An Overview of Structural and Functional Aspects*. *Madame Curie Bioscience Database [Internet]* (Landes Bioscience, 2013).
64. Campbell, I. D. & Humphries, M. J. Integrin structure, activation, and interactions. *Cold Spring Harb Perspect Biol* **3**, a004994 (2011).
65. Miyazaki, Y. *et al.* Integrin αDβ2 (CD11d/CD18) is expressed by human circulating and tissue myeloid leukocytes and mediates inflammatory signaling. *PLoS One* **9**, e112770 (2014).
66. Ammon, C. *et al.* Comparative analysis of integrin expression on monocyte-derived macrophages and monocyte-derived dendritic cells. *Immunology* **100**, 364–369 (2000).
67. Schittenhelm, L., Hilkens, C. M. & Morrison, V. L. β2 Integrins As Regulators of Dendritic Cell, Monocyte, and Macrophage Function. *Frontiers in Immunology* **8**, (2017).
68. Bachmann, M., Kukkurainen, S., Hytönen, V. P. & Wehrle-Haller, B. Cell Adhesion by Integrins. *Physiological Reviews* **99**, 1655–1699 (2019).
69. Arnaout, M. A., Goodman, S. L. & Xiong, J.-P. Structure and mechanics of integrin-based cell adhesion. *Curr Opin Cell Biol* **19**, 495–507 (2007).
70. Podolnikova, N. P., Podolnikov, A. V., Haas, T. A., Lishko, V. K. & Ugarova, T. P. Ligand recognition specificity of leukocyte integrin αMβ2 (Mac-1, CD11b/CD18) and its functional consequences. *Biochemistry* **54**, 1408–1420 (2015).
71. Geiger, B., Bershadsky, A., Pankov, R. & Yamada, K. M. Transmembrane crosstalk between the extracellular matrix--cytoskeleton crosstalk. *Nat Rev Mol Cell Biol* **2**, 793–805 (2001).
72. Girard-Lauriault, P.-L. *et al.* Adhesion of Human U937 Monocytes to Nitrogen-Rich Organic Thin Films: Novel Insights into the Mechanism of Cellular Adhesion. *Macromolecular Bioscience* **9**, 911–921 (2009).
73. Horzum, U., Ozdil, B. & Pesen-Okvur, D. Step-by-step quantitative analysis of focal adhesions. *MethodsX* **1**, 56–59 (2014).
74. Sand, K. M. K. *et al.* Dissection of the neonatal Fc receptor (FcRn)-albumin interface using mutagenesis and anti-FcRn albumin-blocking antibodies. *J Biol Chem* **289**, 17228–17239 (2014).
75. Zhu, X. *et al.* MHC Class I-Related Neonatal Fc Receptor for IgG Is Functionally Expressed in Monocytes, Intestinal Macrophages, and Dendritic Cells. *The Journal of Immunology* **166**, 3266–3276 (2001).
76. Bellis, S. L. Advantages of RGD peptides for directing cell association with biomaterials. *Biomaterials* **32**, 4205–4210 (2011).
77. Conformational equilibria and intrinsic affinities define integrin activation. *The EMBO Journal* **36**, 629–645 (2017).
78. Murthy, S., Kozbial, A. & Bergeron, A. automated dendritic cell generation in a closed system. *Cytotherapy* **22**, S38 (2020).
79. Rezzonico, R., Chicheportiche, R., Imbert, V. & Dayer, J.-M. Engagement of CD11b and CD11c β2 integrin by antibodies or soluble CD23 induces IL-1β production on primary human monocytes through mitogen-activated protein kinase–dependent pathways. *Blood* **95**, 3868–3877 (2000).
80. Reyes-Reyes, M., Mora, N., Gonzalez, G. & Rosales, C. beta1 and beta2 integrins activate different signalling pathways in monocytes. *Biochem J* **363**, 273–280 (2002).

81. Togashi, D. M., Ryder, A. G. & Heiss, G. Quantifying adsorbed protein on surfaces using confocal fluorescence microscopy. *Colloids Surf B Biointerfaces* **72**, 219–229 (2009).
82. Ahmad Khalili, A. & Ahmad, M. R. A Review of Cell Adhesion Studies for Biomedical and Biological Applications. *Int J Mol Sci* **16**, 18149–18184 (2015).

APPENDIX

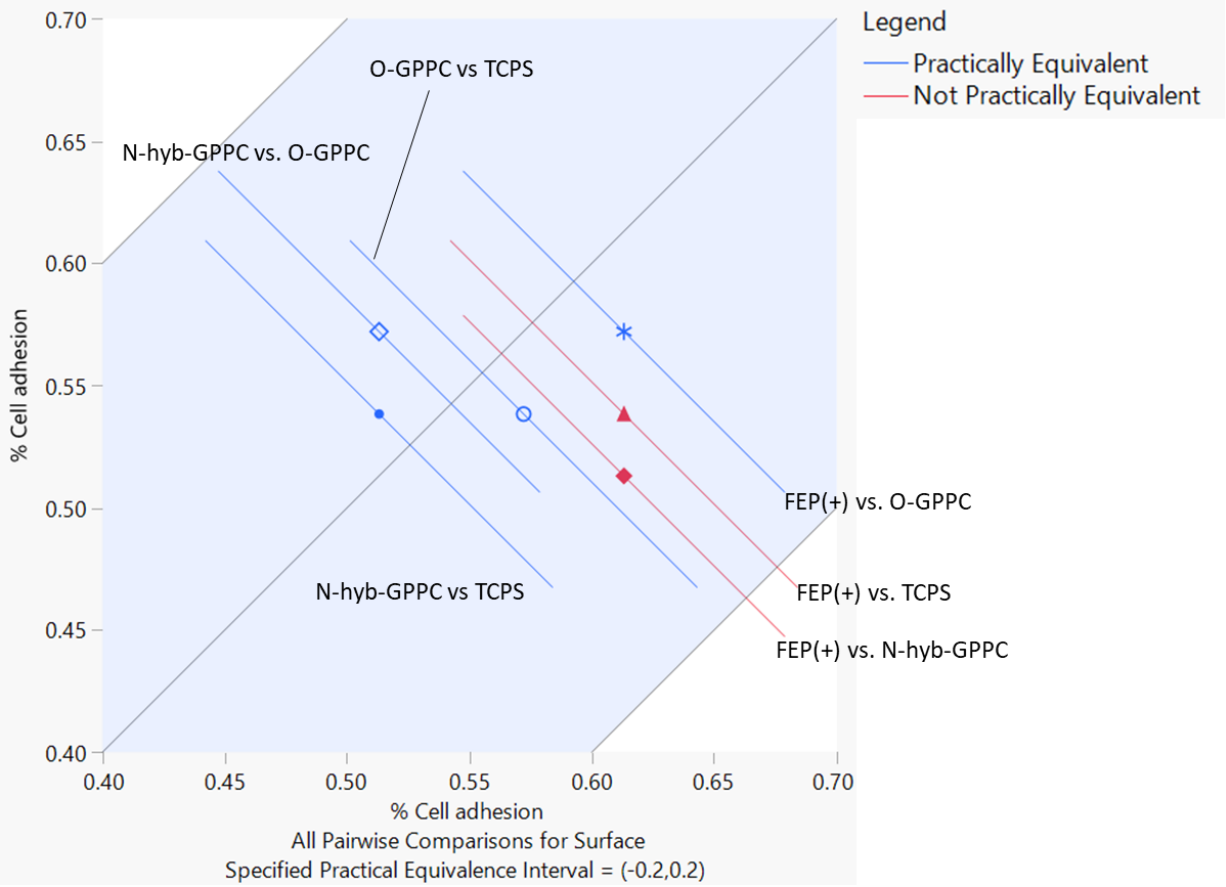

Figure S-0-1 Two one-sided t-tests (TOST) equivalence tests of cell adhesion on TCPS(+), FEP(-), FEP(+), O-GPPC and N-hyb-GPPC at 2h with a zone of indifference of 20% and confidence level of 95%. Test performed with JMP Pro 16.1.0.